The Monte Carlo method in lattice gauge theories

Yu. M. Makeenko

Institute of Theoretical and Experimental Physics, Moscow

Usp. Fiz. Nauk **143**, 161–212 (June 1984)

Applications of the Monte Carlo method in lattice gauge theories, including applications in quantum chromodynamics, are reviewed. The lattice formulation of gauge theories, the corresponding concepts, and the corresponding methods are introduced. The Monte Carlo method as it is applied to lattice gauge theories is described. Some specific calculations by the Monte Carlo method and their results are examined. The phase structure of lattice gauge theories with Abelian groups Z_N and U(1) (a lattice formulation of a compact electrodynamics) is discussed. The non-Abelian groups SU(2), SU(3) (a lattice formulation of quantum chromodynamics), and others are also discussed. The procedure for calculating quantities referring to the continuum limit by the Monte Carlo method is discussed for quantum chromodynamics. A detailed analysis is made of results calculated for the continuum theory: string tensions and interaction potentials, which show that quarks are confined; glueball mass spectra; and the temperature of the transition from the phase of hadronic matter to the phase of a quark-gluon plasma. Masses calculated for hadrons consisting of quarks are briefly discussed.

TABLE OF CONTENTS

INTRODUCTION

Quantum chromodynamics (QCD), proposed in its modern form just over a decade ago by Gell-Mann, Fritzsch, and Weinberg,[1] has now become the generally accepted theory of the strong interaction. In QCD the interaction between quarks is associated with their color and is implemented by an octet of gluon fields (see Ref. 2, for example). The most important property of QCD, which was pointed out by Gross, Wilczek, and Politzer,[3] is the property of asymptotic freedom (the effective interaction constant is small at short range). Because of this property, perturbation theory can be used for calculations for processes determined by short distances in QCD.

With increasing distance the effective interaction constant increases, however, so that quantities determined by

 0038-5670/84/060401-30$01.80

distances over which the interaction actually becomes strong cannot be caculated by perturbation theory. Among these quantities are most of the quantities which arise in the theory of the strong interaction, e.g., those which pertain to low-energy hadron physics (hadron masses, decay widths, interaction cross sections, etc.). In order to calculate these quantities it is necessary in principle to consider not only a perturbation-theory series in a coupling constant (perturbative QCD) but also—and more importantly!—the nonperturbative contributions, which do not arise in any order of perturbation theory.

It nevertheless turns out that in QCD there is a certain interval of intermediate distances over which these nonperturbative contributions can be described in a simple way by altering the structure of the QCD vacuum: by incorporating gluon and quark condensates in the vacuum. These condensates are determined in succession through an operator expansion (an expansion in powers of the product of the distance R and the scale dimension of the strong interaction, Λ_{QCD}). This expansion makes it possible to calculate the contributions of these condensates to physical quantities. Incorporating gluon and quark condensates improves the QCD description of several physical processes, making it possible in particular to derive reliably, by a sum-rule method, the masses and widths of the mesons of the J/ψ family[4] and also the masses of the lower mesons[5] and baryons[6] which are made up of light quarks.

In QCD there are also many phenomena which are governed by large distances, $R\Lambda_{\text{QCD}} > 1$, where the operator expansion (not to mention perturbation theory) cannot be used. Among these phenomena are quark confinement and the appearance in QCD of the string, bag, Regge-trajectory, and other models. These phenomena do not arise in any finite order of a perturbation theory in the coupling constant; they are due entirely to nonperturbative effects. One more example of phenomena of this type is the appearance of quark and gluon condensates. Consequently, although it is expected that these phenomena have a place in the theory of the strong interaction, nonperturbative methods must be used to derive them from the QCD Lagrangian.

In this review we will examine a relatively new nonperturbative method, which is based on a numerical integration by the Monte Carlo method of QCD regularized in a special way by means of a lattice. The Monte Carlo method has the advantage over other nonperturbative methods which have been developing in parallel (for example, the method of reducing QCD to the theory of a relativistic string[7]) that the calculations can more frequently be carried out completely, and their results can be compared with experiment. Let us list the basic steps which must be taken in Monte Carlo calculations in QCD.

We use a formulation of QCD involving a functional integral. For this formulation an average over quantum fluctuations of the fields at each point in space-time is represented as an explicit integral (see Ref. 8, for example). From this point on the idea is, roughly speaking, to evaluate these integrals numerically using the Monte Carlo method.

A transformation is made to Euclidean space; i.e., the time t is replaced by a fourth coordinate x_4 in accordance with $x_4 = it$. This procedure is used frequently in perturbation theory to simplify the calculations. This procedure is also standard in the nonperturbative formulation of the theory; it leads to a convergence of the functional integral at each point in Euclidean space. If some quantity, say a Green's function, is calculated in the Euclidean theory, then its value in a theory defined in Minkowski space is obtained by using the analytic continuation $t = -ix_4$ (see Ref. 9, for example). This approach can of course be used to find only quantities in the space-like part of Minkowski space; it cannot be used, for example, to find a form factor in the time-like region. We are still able to calculate the interaction potential between static quarks, the hadron mass spectrum, and some other quantities which we will be discussing below.

The continuous Euclidean space is replaced by a discrete set of points: a lattice. The introduction of a lattice makes the functional integral a correctly defined quantity and allows us to calculate this integral by the methods of statistical physics. Although, by virtue of its construction, a theory formulated on a lattice is not invariant under the rotation group or the displacement group (all that remains are discrete symmetries under rotations through angles which are multiples of $\pi/2$ and under displacements by a multiple of the lattice spacing), these symmetries are present in the final results if the scale dimension for changes in the fields is much greater than the lattice spacing. For this purpose, the coupling constant in the lattice theory is chosen near the point of a second-order phase transition (at a second-order phase transition, the correlation length becomes infinite). It is this situation with which we deal in Monte Carlo calculations in QCD, so that it is possible to obtain results on the continuum limit from calculations on a lattice.

More specifically, the following procedure is used. The introduction of a lattice ensures an appropriate ultraviolet regularization of the quantum theory. If the spatial dimension of the lattice is bounded (this would mean an infrared regularization), then the system on the whole has a finite number of degrees of freedom, so that all the results calculated for dimensional quantities which are expressed in units of the lattice spacing are finite. If these quantities are to refer to the continuum limit, they must depend on the coupling constant in a certain way prescribed by the renormalizability of QCD (see the equations in Subsection 4a). Another important point is that the quantities which are calculated should not depend on the spatial dimension of the lattice or on the choice of boundary conditions which are imposed on the field at the boundary. Luckily, it turns out that the scale dimension for changes in the fields at which the lattice structure is not sensed is only a few times the lattice spacing, so that even on a lattice no larger than 8^4 the Monte Carlo method can reliably provide results referring to the continuum limit (the multiplicity of the integral which is evaluated in this case is $\approx 10^6$). The lattice must therefore be perceived as simply a regularization method which makes it possible to obtain results for the continuum theory.

As we have already mentioned, the most interesting of the results obtained by this method are those which stem from nonperturbative effects and which cannot be derived by perturbation theory. Monte Carlo calculations have

shown that the Coulomb interaction potential between static quarks gives way with increasing distance to a linearly increasing potential, which results in the confinement of quarks. The value calculated for the parameter Λ_{QCD} in this case agrees with the phenomenological value. Furthermore, the Monte Carlo method has been used to calculate the mass spectrum of colorless gluon formations—glueballs—and hadrons made up of quarks. The values of the gluon and quark condensates and other quantities which arise in QCD have also been calculated. A separate group of studies has been devoted to calculations in QCD at a finite temperature. Here the Monte Carlo method has been used to calculate that temperature (T_c) at which a phase transition occurs from a phase of hadronic matter to a phase of a quark-gluon plasma, in which quarks are not confined. The Monte Carlo method has also been used to calculate the temperature at which the quark condensate is destroyed and a variety of characteristics of the quark-gluon plasma.

For comparison with experiment we need to know the accuracy of the Monte Carlo calculations. The error of these calculations consists of the statistical error, which decreases with increasing computation time, as in all Monte Carlo calculations, and various systematic errors which stem from the particular approximations which are used, including the usual approximation of ignoring the contribution of virtual quarks to physical quantities. For calculations of hadron masses by this method, for example, the total error is estimated to be about $\pm$ 150 MeV. The agreement with experiment is within this error, although this error is quite large. At any rate, these values are obtained directly from the first principles of QCD without any appeal to additional hypotheses, and their agreement with experiment may be regarded as a test of QCD at low energies. Certain other results of Monte Carlo calculations, such as glueball masses and the value of T_c, are predictions for the future.

We will examine in detail how the Monte Carlo method is used to study lattice gauge theories, including QCD without quarks. The two goals of this review are to introduce the reader to the concepts and methods presently used in research on the dynamics of gauge theories and to review the basic results which have emerged from the vast number of published studies in this field. As the title of this review implies, we will be discussing in greatest detail the Monte Carlo method and the results which have been obtained by this method. We will reproduce several figures from the original papers with results calculated by the Monte Carlo method.

In Section 1 we list the basic concepts of lattice gauge theories. We discuss the lattice formulation of gauge theories, the quantization of lattice gauge theories by the functional-integral method, the Wilson quark-confinement criterion, and the appearance of an area law in the strong-coupling limit. We examine the question of which renormalization factors must be separated from the quantities of interest when we take the continuum limit.

Section 2 describes the Monte Carlo method as it is applied to lattice qauge theories. We discuss some specific algorithms which have been used for calculations: the heat bath method and the Metropolis method.

Section 3 uses the simple example of calculating the specific energy for a detailed look at the procedure for using the Monte Carlo method in research in lattice gauge theories. We examine the problem of choosing an initial state and the relaxation to equilibrium. We discuss quantities which are calculated in order to answer the question of whether a given gauge system undergoes a phase transition, and if so, of what order. We look at some results obtained by this method for lattice theories with the Abelian gauge groups Z_N and U(1) and also with the non-Abelian gauge groups SU(N) and U(N), among others. We discuss the nature of the physical phenomena which occur at the points of phase transitions.

Section 4 reviews the results derived by the Monte Carlo method in continuum QCD (without quarks). We see how the continuum limit is taken in QCD calculations by the Monte Carlo method. We look at results calculated on the string tension, glueball masses, and the temperature T_c. We discuss the extent to which these results are independent of the particular choice of action in the lattice gauge theory.

This review is restricted to Monte Carlo calculations in QCD without quarks. To include also the results obtained for QCD with quarks would have substantially increased the length of this review. Furthermore, at this stage the work on QCD with quarks is comparatively incomplete. References to this other work are given in the Conclusion.

1. LATTICE GAUGE THEORIES

Lattice gauge theories in their modern form were proposed in 1974 by Wilson[10] and independently by Polyakov (his work was published in Ref. 11). Wegner's study[12] of an Ising gauge model is also cited frequently in this connection. A Hamiltonian formulation was developed by Kogut and Susskind.[13] In addition, the papers by Balian, Drouffe, and Itzykson[14] and Migdal[15] have had considerable influence on the subsequent development of lattice gauge theories.

Lattice gauge theories constitute a nonperturbative regularization of a gauge theory. The lattice formulation also has several other advantages. The problem of a nonperturbative quantization of the gauge theories can be solved in a simple and elegant way on a lattice. The lattice formulation allows a strong-coupling expansion, in each order of which quarks are confined. Finally, a lattice gauge theory can be studied by the Monte Carlo method at arbitrary values of the coupling constants.

a) Lattices, links, plaquettes, and all that

The first step in constructing a lattice gauge theory is to approximate the continuous space by a discrete set of points: a lattice. In the Euclidean formulation, the lattice is introduced along all four coordinates. In the Hamiltonian approach, the time is left continuous. Here we will discuss only the Euclidean formulation, for which the Monte Carlo method is used.

A "lattice" is defined as a set of spatial points with the coordinates

$$x_\mu = an_\mu, \tag{1.1}$$

where the components of the vector

$$n_\mu = (n_x, n_y, n_z, n_t) \tag{1.2}$$

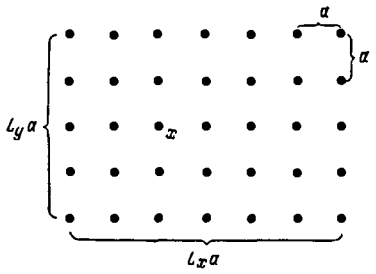

FIG. 1. Two-dimensional lattice.

are the natural numbers. Points (1.1) are called "lattice sites." The dimensional constant a, equal to the distance between neighboring sites, is called the "lattice spacing." Dimensional quantities will usually be expressed in units of a, so that we would have $a = 1$. Figure 1 shows a two-dimensional lattice. A four-dimensional lattice for which the distances between sites are identical in all directions (as for the lattice shown here) is called a "hypercubic lattice."

The next concept is the "link" of a lattice. A link is a line which connects two neighboring sites. A link is denoted by the letter "l" (or "b") and is characterized by the coordinate (x) of its starting point and its spatial direction $\mu = 1,\ldots, 4$ ($\mu = 1$ represents the x axis; . . .; and $\mu = 4$ represents the t axis):

$$l = \{x, \ \mu\}. \tag{1.3}$$

A link l joins sites with coordinates x and $x + a\hat{\mu}$, where $\hat{\mu}$ is a unit vector along the μ direction, as shown in Fig. 2. For a hypercubic lattice, the lengths of all links are equal to a.

The elementary square enclosed by four links is a "plaquette." A plaquette p is specified by the coordinate (x) of a site on which a square is constructed along the μ, ν direction (Fig. 3):

$$p = \{x; \ \mu, \nu\}. \tag{1.4}$$

The set of four links which form the boundary of a plaquette p is denoted by ∂p (or, less frequently, $\dot{p}$).

If the spatial dimension of the lattice is not bounded, then the number of dynamic degrees of freedom is infinite (but denumerable). Monte Carlo calculations can in practice be carried out with a large but finite number of degrees of freedom. To limit the number of degrees of freedom, one deals with a lattice which has finite dimensions in all directions: $L_x \times L_y \times L_z \times L_t$ (Fig. 1). "Periodic boundary conditions" are imposed; i.e., pairs of sites which lie on parallel bounding hyperplanes are identified with each other [the sites with coordinates $(0, n_y, n_z, n_t)$ and (L_x, n_y, n_z, n_t), for example, are identified with each other].

For a symmetric lattice ($L_x = L_y = L_z = L_t = L$) with periodic boundary conditions, the numbers of independent

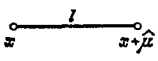

FIG. 2. A link of a lattice.

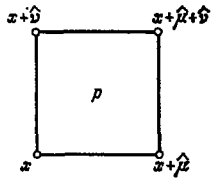

FIG. 3. A plaquette of a lattice.

sites, links, and plaquettes are, respectively,

$$N_s = L^d, \quad N_l = dL^d, \quad N_p = \frac{d(d-1)}{2} L^d, \tag{1.5}$$

where $d = 4$ is the dimensionality of the space.

b) Gauge fields on a lattice

In the continuum theory the gluon field is described by the vector potential[1,2] $A_\mu^a(x)$. It is convenient to multiply this potential by the generator (t^a) of a fundamental representation of the gauge group and to work with the Hermitian matrix

$$A_\mu(x) = A_\mu^a(x)\, t^a, \tag{1.6}$$

which is an element of the algebra of the gauge group. The nonAbelian field then becomes

$$F_{\mu\nu}(x) = \partial_\mu A_\nu(x) - \partial_\nu A_\mu(x) - ig_0 [A_\mu(x), A_\nu(x)], \tag{1.7}$$

where g_0 is the charge of the gluon field.

On a lattice the gluon field is described by matrices $U_{x,\mu}$ which are assigned to the links of the lattice. The $U_{x,\mu}$ are elements of the gauge group itself. The matrix $U_{x,\mu}$ can be represented as an exponential function of the μth component of the vector potential. For this purpose we note that the quantity on the right side of the relation

$$U_{x,\mu} = 1 + ig_0 A_\mu(x)\, a + O(a^2) \tag{1.8}$$

is, to an accuracy $O(a^2)$, an element of the gauge group. In other words, under a local gauge transformation

$$A_\mu(x) \to \Omega^{-1}(x) A_\mu(x) \Omega(x) + \frac{i}{g_0} \Omega^{-1}(x) \partial_\mu \Omega(x) \tag{1.9}$$

it transforms homogeneously within the specified error:

$$U_{x,\mu} \to \Omega_x^{-1} U_{x,\mu} \Omega_{x+\hat{\mu}}. \tag{1.10}$$

For a proof, we need to replace the derivative in (1.9) by a finite difference. The matrix Ω_x is equal to the value of the matrix $\Omega(x)$ at the lattice sites.

It is now clear how we are to establish the exact relationship between the matrices $U_{x,\mu}$ and $A_\mu(x)$. We partition the link between the points x and $x + a\hat{\mu}$ into infinitesimally small parts, for which Eq. (1.8) is valid, and we define $U_{x,\mu}$ as an ordered matrix product (here the matrices are ordered from left to right, in the order in which the link goes from the point x to the point $x + a\hat{\mu}$):

$$U_{x,\mu} = \prod_{1}^{j=L} \left[1 + ig_0 A_\mu\left(x + \frac{j}{L} a\hat{\mu}\right) \frac{a}{L}\right]. \tag{1.11}$$

Since each cofactor transforms homogeneously under a gauge transformation, the matrices Ω cancel out at the inte-

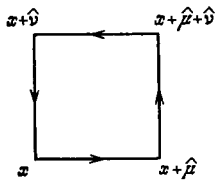

FIG. 4. A contour in the form of an oriented boundary of a plaquette.

rior points of a link, and the matrix $U_{x,\mu}$ defined by (1.11) transforms exactly in accordance with Eq. (1.11) under a gauge transformation [but now this is true in any order in a, not simply $O(a^2)$, as before]. The quantity on the right side of (1.11) is an "ordered phase factor." For it there is a special notation:

$$U_{x,\mu} = P\exp\left[ig_0 \int_x^{x+a\hat{\mu}} A_\mu(\xi)\, d\xi_\mu\right]. \tag{1.12}$$

This is the final expression which relates the lattice matrix $U_{x,\mu}$ to the potential $A_\mu(x)$ in the continuum theory.

It can be seen from (1.12) that the concept of the orientation of a given link arises in a lattice gauge theory. The orientation of a link is the direction in which the matrices in the contour integral are ordered. Above we characterized a link $\{x,\mu\}$ by the coordinate (x) of its starting point and the (positive) direction μ. We now assume a link has a negative direction, $-\mu$, if its direction is opposite the direction of the μth axis. Consequently, both the link $\{x, \mu\}$ and the link $\{x+\hat{\mu}, -\mu\}$ connect the points x and $x+\hat{\mu}$, but in the former case the orientation of the link is positive (it is the same as the direction of the coordinate axis), while in the latter case it is negative. The matrices U which are assigned to links with positive and negative orientations are related in case of unitary matrices by

$$U_{x+\hat{\mu},\,-\mu} = U^+_{x,\,\mu}. \tag{1.13}$$

The phase-factor definition in (1.12) can be generalized without any difficulty to an arbitrary contour. In the construction of a lattice gauge theory, the most important role is played by the simplest closed contour: the boundary of a plaquette, as shown in Fig. 4. Here the arrows show the order in which the matrices $U_{x,\mu}$ are multiplied. This contour corresponds to the ordered product

$$U_p = U_{x,\,\mu} U_{x+\hat{\mu},\,\nu} U^+_{x+\hat{\nu},\,\mu} U^+_{x,\,\nu}. \tag{1.14}$$

In constructing it we made use of property (1.13). It follows from (1.10) that under a gauge transformation U_p transforms in accordance with

$$U_p \to \Omega_x^{-1} U_p \Omega_x. \tag{1.15}$$

Consequently, the trace of the matrix U_p is gauge-invariant. This property is exploited in constructing an action for a lattice gauge theory.

An expression for a phase factor corresponding to an arbitrary contour can be derived by analogy with (1.14). Let us assume that the contour C is specified by its initial point x and by the directions (some of which may be negative) of the adjoining links:

$$C = \{x, \mu_1, \ldots, \mu_n\}. \tag{1.16}$$

The matrix U_C is constructed in accordance with the rules above:

$$U_C = U_{x,\,\mu_1} U_{x+\hat{\mu}_1,\,\mu_2} \ldots U_{x+\hat{\mu}_1+\ldots+\hat{\mu}_{n-1},\,\mu_n}. \tag{1.17}$$

For the links with a negative direction it is convenient to make use of property (1.13) again. The only gauge-invariant trace of contour products is that for closed contours, with $\hat{\mu}_1 + \ldots + \hat{\mu}_n = 0$. Expressions of this type are used in calculating physical quantities.

c) Lattice action. "Naive" local limit

The action of any lattice theory can be derived from the action of the continuum theory by replacing the derivatives [which appear in the field (1.7), for example] by finite differences and replacing the integrals by sums over the lattice sites. For a gauge theory, however, this quantization procedure is correct only in the free case; for a gauge theory with an interaction, this procedure would violate the local gauge invariance. Consequently, in constructing the action of a lattice gauge theory one uses the formulation of the preceding subsection, for which the gauge fields are assigned to links of the lattice rather than to sites.

The Wilson action of a U(N) lattice gauge theory is constructed through the use of a simple gauge-invariant quantity $\mathrm{tr}\,U_p$:

$$S(U) = \sum_p \left(1 - \frac{1}{N}\,\mathrm{Re}\,\mathrm{tr}\,U_p\right). \tag{1.18}$$

The summation is over all the elementary plaquettes of the lattice (i.e., over all x, μ, and ν), regardless of their orientations. Since $\mathrm{tr}\,U_p$ converts into its complex conjugate upon a reversal of the orientation of a plaquette, by virtue of property (1.13),

$$\mathrm{tr}\,U_p \xrightarrow[\text{reorientation}]{} (\mathrm{tr}\,U_p)^*, \tag{1.19}$$

we can also rewrite action (1.18) in the equivalent form

$$S(U) = \frac{1}{2} \sum_{\text{oriented } p} \left(1 - \frac{1}{N}\,\mathrm{tr}\,U_p\right), \tag{1.20}$$

where the sum is also over the two possible orientations of a given plaquette.

In the limit $a \to 0$ the lattice action (1.18) becomes the action of a U(N) continuum gauge theory. To see this, we note that in the limit $a \to 0$ we have

$$U_p = \exp\left[ig_0 F_{\mu\nu}(x)\, a^2 + O(a^3)\right], \tag{1.21}$$

where $F_{\mu\nu}$ is defined by (1.7). In an Abelian theory, expansion (1.21) is easily found from the Stokes theorem. The commutator of $A_\mu(x)$ and $A_\nu(x)$ which arises in the non-Abelian case complements the Abelian field to a non-Abelian field, as is ensured by the gauge invariance.

The transition to the continuum limit is accomplished by means of

$$a^4 \sum_p \xrightarrow[a\to 0]{} \frac{1}{2} \int d^4x \sum_{\mu,\,\nu}. \tag{1.22}$$

Expanding the exponential function in (1.21) in a series we

find

$$S(U) \xrightarrow[a\to 0]{} \frac{g_0^2}{2N} \int d^4x \sum_{\mu,\nu} \operatorname{tr} F_{\mu\nu}^2(x). \tag{1.23}$$

That the action is a scalar can be seen after summing over μ and ν.

The lattice action (1.18) converts into the action of the continuum theory in the limit $a\to 0$ (at a fixed g_0). This limit is known as the "naive" local limit in quantum field theory. By analogy with the action, other quantities used in the lattice gauge theory, U_C, for example, convert in the naive local limit into the corresponding quantities for the continuum theory.

d) Quantization of gauge fields on a lattice

In the continuum theory a gauge field can be quantized through the use of functional integrals

$$\int_{-\infty}^{+\infty} \cdots \int_{-\infty}^{+\infty} \prod_x \prod_\mu \prod_a dA_\mu^a(x) \exp\left[-\frac{1}{2}\int d^4x \operatorname{tr} F_{\mu\nu}^2(x)\right]; \tag{1.24}$$

here the number of independent integrations (the number of degrees of freedom) is

$$N_s\, d\, d_G, \tag{1.25}$$

where N_s is the number of points in the space, d is the dimensionality of the space, and d_G is the dimensionality of the gauge group [$d_G = N_c^2 - 1$ for the SU(N_C) group]. For each of these integrals to converge, it is necessary to work in a Euclidean space, in which the action appears in the argument of the exponential function with a minus sign. In order to assign a mathematical meaning to functional integral (1.24) we must also restrict the discussion to a denumerable set of spatial points; e.g., we could use the lattice approximation.[16]

In a lattice gauge theory using the matrices $U_{x,\mu}$ as dynamic variables, the funtional integral (1.24) is replaced by a functional integral of the type

$$Z(\beta) = \int \prod_{x,\mu} dU_{x,\mu} e^{-\beta S(U)}. \tag{1.26}$$

As the action we can take any gauge-invariant expression which converts in the limit $a\to 0$ into the action of the continuum theory. The simplest action is the Wilson action (1.18), and this is the one most commonly used. A subtler question is how the measure of the integration changes when we adopt the lattice approximation. In expression (1.26) the integration is over an invariant "group measure" or "terHaar measure." Invariance of the group measure under multiplication form the left or right by an arbitrary element of the group

$$dU = d(\Omega U) = d(U\Omega) \tag{1.27}$$

guarantees gauge invariance of the functional integral (1.26).

To examine an explicit expression for the group measure we consider the case of the SU(2) gauge group. Any arbitrary element of the SU(2) group can be parametrized by means of the unit three-vector $\mathbf{n}$ ($\mathbf{n}^2 = 1$) and the angle $\varphi(\varphi\in[0,2\pi])$:

$$U = e^{i\varphi \mathbf{n}\sigma/2} = \cos\frac{\varphi}{2} + i\mathbf{n}\sigma \sin\frac{\varphi}{2}; \tag{1.28}$$

here the σ are the Pauli matrices. The geometric meaning of this parametrization is extremely simple: An element (1.28) corresponds to a rotation through an angle φ around the $\mathbf{n}$ axis.

For practical calculations it is convenient to form the unit four-vector

$$a_\mu = \left(\mathbf{n}\sin\frac{\varphi}{2}, \cos\frac{\varphi}{2}\right), \quad a_\mu^2 \equiv \sum_{\mu=1}^{4} a_\mu^2 = 1, \tag{1.29}$$

which puts expansion (1.28) of the matrix U in the basis of the four matrices $\sigma_\mu = (i\sigma, I)$ in the simple form

$$U = a_\mu \sigma_\mu, \quad a_\mu = \frac{1}{2}\operatorname{tr}\sigma_\mu U. \tag{1.30}$$

An integration over the terHaar measure for the SU(2) group can be represented as an integration over an element of solid angle in the four-dimensional space by one of the two equivalent methods

$$dU = \frac{d^2\mathbf{n}}{4\pi}\frac{d\varphi}{\pi}\sin^2\frac{\varphi}{2}, \tag{1.31a}$$

$$dU = \frac{d^4a_\mu}{\pi^2}\delta(a_\mu^2 - 1). \tag{1.31b}$$

Expression (1.31a) is found from (1.31b) by taking the integral of the δ-function over $|\mathbf{a}|$. The condition $a_\mu^2 = 1$ which arises in the course of this integration is equivalent to the conditions that the matrix U must be unitary and unimodular, since for representation (1.30) we have $UU^+ = a_\mu^2 I$ and $\det U = a_\mu^2$.

As always, the quantity $Z(\beta)$ defined by the functional integral (1.26) characterizes vacuum effects in the quantum theory. To calculate physical quantities we must average gauge-invariant functionals $Q[U]$ over the field U:

$$\langle Q[U]\rangle = Z^{-1}(\beta)\int \prod_{x,\mu} dU_{x,\mu} e^{-\beta S(U)} Q[U]. \tag{1.32}$$

In the naive local limit this expectation value becomes the corresponding expectation value of the continuum theory if the constant β is related to the charge g_0^2 by

$$g_0^2 = \frac{2N_c}{\beta}, \tag{1.33}$$

a relation which follows from (1.23).

On a lattice of finite size the integrals over the group in (1.32) are bounded, since the integration is carried out over a compact group manifold, and no infinity arises from the volume of the gauge group. Expression (1.32) is thus a constructive method for calculating expectation values of gauge-invariant quantities, although the gauge is not fixed. The gauge can be fixed in the standard way, by the Faddeev-Popov method.[17,8] This procedure involves extracting a (finite) common factor, equal to the volume of the gauge group, from the numerator and denominator in (1.32). A functional integral with a fixed gauge is convenient for calculations in a lattice perturbation theory. A Lorentz gauge cannot be fixed outside a perturbation theory, however, because of Gribov's ambiguities.[18] In contrast, the functional integral (1.32) with an unfixed gauge is a correct nonperturbative quantization method.

The compactness is achieved at the expense of the periodicity in the vector potential [for the U(1) group, for example, values of the vector potential A_μ and $A_\mu + (2\pi/ag_0)$ become identified with each other]; this periodicity does not occur in an ordinary gauge theory since discontinuities of the vector potential in a continuum theory correspond to an infinite action. The lattice analog of these discontinuities would be fluctuations of the vector potential $A_\mu \sim 1/a$, for which the lattice action (1.18) is, however, finite, so that the integration also goes over configurations of this type. The lattice gauge theories are thus not simply a regularization but also a nontrivial, nonperturbative addition to the definition of the perturbation-theory series. Monte Carlo calculations show that fluctuations $A_\mu \sim 1/a$ actually become unimportant when we take the local limit in the case of a four-dimensional non-Abelian theory, in which we are interested here. The actual local limit is thus very similar to the naive limit.

e) Strong-coupling expansion

There are several ways to calculate the functional integral (1.32) approximately. In the very first paper by Wilson[10] an expansion was carried out in the parameter β, which is related to the charge g_0^2 by (1.33). The limit of small values of β (or large values of g_0^2) is called the "strong-coupling limit," and the evaluation of the integral (1.32) as an expansion in β is called a "strong-coupling expansion" or "high-temperature expansion." The latter term stems from the analogy between the functional integral (1.26) and the partition function of some (four-dimensional) system. The constant β is thus an analog of the reciprocal temperature, and the expanson in β is an analog of a high-temperature expansion in statistical physics.

The basic quantity with which we must work in lattice calculations is the "loop average" of the phase factor (1.17):

$$W(C) = \left\langle \frac{1}{N} \operatorname{tr} U_C \right\rangle. \tag{1.34}$$

Here the average is taken in accordance with (1.32).

To calculate $W(C)$ in the strong-coupling limit, we expand the exponential function in a series in β, reducing the problem to one of evaluating the group integrals

$$\int dU\, U^{i_1}_{j_1} \dots U^{i_n}_{j_n} U^{+k_1}_{l_1} \dots U^{+k_m}_{l_m}, \tag{1.35}$$

where the measure is normalized by the condition $\int dU = 1$. We know from general considerations that the integral (1.35) is nonzero only if $n = m(\mathrm{mod}N)$, i.e., only if $n = m + kN$, where k is any integer. For the simplest case $m = n = 1$ the answer can be found easily by making use of the unitarity of the matrices U and the orthogonality relation

$$\int dU\, U^i_j U^{+k}_l = \frac{1}{N} \delta^i_l \delta^k_j. \tag{1.36}$$

These relations are sufficient for evaluating loop averages in the first approximation in β.

Let us examine the simple case of a loop which is the boundary of a plaquette: $C = \partial p$ (Fig. 4). In the β order it is sufficient to retain only the first two terms in the expansion of the exponential function:

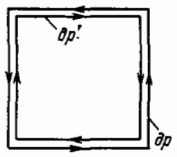

FIG. 5. Boundaries of the plaquettes p and p', which are oppositely oriented.

$$W(\partial p) = \frac{\int \prod\limits_{x,\mu} dU_{x,\mu} \frac{1}{N} \operatorname{tr} U_p \left(1 + \beta \sum\limits_{p'} \frac{1}{N} \operatorname{Re} \operatorname{tr} U_{p'}\right)}{\int \prod\limits_{x,\mu} dU_{x,\mu} \left(1 + \beta \sum\limits_{p'} \frac{1}{N} \operatorname{Re} \operatorname{tr} U_{p'}\right)} + O(\beta^2). \tag{1.37}$$

A group integration is then carried out in accordance with

$$\int dU_l U^i_{lj} U^{+n}_{l'm} = \frac{1}{N} \delta_{l'l} \delta^i_m \delta^n_j, \tag{1.38}$$

which follows from the rules given above. The symbol $\delta_{ll'}$ means that the (oriented) link l' must coincide with the link l if the result of the integration is to be nonzero. According to this rule, the denominator in (1.37) is equal to one (each link is encountered no more than once), while in the numerator the only nonvanishing contribution is that from plaquette p', which coincides with plaquette p but has the opposite orientation [see Fig. 5 and Eq. (1.19)]. Multiplication of the Kronecker deltas finally gives us

$$W(\partial p) = \frac{\beta}{2N^2} \quad \text{for the SU}(N)\text{ group with } N \geqslant 3, \tag{1.39a}$$

$$W(\partial p) = \frac{\beta}{4} \quad \text{for the SU(2) group.} \tag{1.39b}$$

The reason for the absence of the additional factor of 1/2 in the case of the SU(2) group is that in this case $\operatorname{tr} U_p$ is real, and the orientation of the plaquettes can be ignored.

Relation (1.38) can also be used to evaluate the first nonvanishing order of the strong-coupling expansion for the loop average in the case of more complex loops. According to (1.38), the only nonvanishing integral is that of a term in the expansion of the exponential function in β for which the plaquettes completely cover a surface bounded by the given loop C (Fig. 6). In this case each link in the group integral is encountered twice (or never), once in the positive direction and once in the negative direction, and all the group integrals are nonzero. The first nonvanishing order corresponds to the coverage of a "minimal surface," whose area takes on the smallest possible value. For the loop average (of a simple

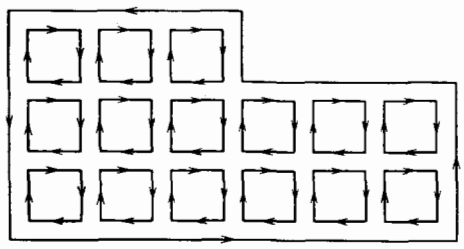

FIG. 6. Filling of a loop with elementary plaquettes.

loop without self-intersections) we thus find, in first order in β,

$$W(C) = [W(\partial p)]^{A_{\min}(C)}, \tag{1.40}$$

where $A_{\min}(C)$ denotes the area (in units of a^2) of the minimal surface bounded by loop C, and $W(\partial p)$ is given by (1.39).

f) Area law

The exponential nature of the dependence of the loop average on the area is called the "area law." It is customary to assume that if an area law holds for large-area loops in pure gluon dynamics then quarks are confined (i.e., there are no physical $|\text{in}>$ or $|\text{out}>$ states). This assertion is the essence of Wilson's "confinement criterion." The argument is that in the case the physical amplitudes, e.g., the polarization operator, have no physical quark singularity.[10]

Another, possibly oversimplified justification for the Wilson criterion is based on the relationship between the loop average and the potential energy of the interaction between static quarks. To find this relationship we consider a loop consisting of a rectangle of dimensions $R \times T$ lying in the x, t plane (Fig. 7). We fix the gauge by means of the condition $A_4(x, \ldots, t) = 0$. We then have

$$W(R, T) = \langle \operatorname{tr} \Psi(0)\, \Psi^+(T) \rangle, \tag{1.41}$$

where

$$\Psi(0) = P \exp \int_0^R A_1(x, \ldots, 0)\, dx,$$
$$\Psi(T) = P \exp \int_0^R A_1(x, \ldots, T)\, dx. \tag{1.42}$$

Substituting into (1.41) a sum over intermediate states,

$$\langle \operatorname{tr} (\Psi(0)\, \Psi^+(T)) \rangle = \sum_n \langle \Psi_{ij}(0)\, |n\rangle \langle n| \Psi_{ji}^{\dagger}(T) \rangle \tag{1.43}$$

and noting that

$$\Psi(T) = e^{-\hat{H}T} \Psi(0)\, e^{\hat{H}T}, \tag{1.44}$$

where the operator H performs a discrete displacement along the "time" axis (the "Hamiltonian" of the system), we finally find

$$W(R, T) = \sum_n |\langle \Psi_{ij}(0)|n\rangle|^2 e^{-E_n T}; \tag{1.45}$$

where E_n is the energy of the $|n>$ state of the system.

We now consider the limit $T \gg R$. In the limit $T \to \infty$ we are left in the sum over states with only the ground state, with the lowest energy and we find

$$W(R, T) \xrightarrow[T\to\infty]{} e^{-E_0(R)T}. \tag{1.46}$$

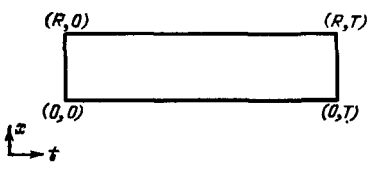

FIG. 7. Rectangular loop of dimensions $R \times T$.

Accordingly, $E_0(R)$ is by definition the change in the energy of the ground state of the lattice system upon the incorporation of static quarks, i.e., the energy of their interaction (including self-effects). The fact that $E_0(R)$ is calculated with the help of a Euclidean functional integral is unimportant in the limit $T \to \infty$. Expression (1.45) could be continued analytically into the Minkowski space without any difficulty by using the replacement $T \to -iT$; it then follows immediately that $E_0(R)$ is a physical energy. As always, the advantage of working in a Euclidean space is that the sum (1.45) converges for all $T > 0$.

By definition, $E_0(R)$ includes a term which stems from the renormalization of the mass of a heavy quark due to the interaction with the gauge field and which is thus independent of R. In the limit $a \to 0$, in first order in g_0^2, this quantity has the same form as in quantum electrodynamics:

$$\Delta E_{\text{mass}} = \frac{g_0^2}{4\pi a} \frac{N_c^2 - 1}{2N_c}. \tag{1.47}$$

The potential energy of the interaction between the static quarks is defined as the difference

$$E(R) = E_0(R) - \Delta E_{\text{mass}}. \tag{1.48}$$

If ΔE_{mass} did not become infinite in the continuum limit ($a \to 0$), the term resulting from the mass renormalization would not have to be subtracted, since it simply changes the reference level for the potential energy.

If the area law

$$W(C) \underset{\text{large } C}{\propto} \exp[-KA_{\min}(C)] \tag{1.49}$$

holds for the loop average, as it does in the strong-coupling expansion, then E is a linear function of the distance:

$$E(R) = KR. \tag{1.50}$$

The coefficient K in these equations is called the "string tension" because the gluon field between quarks must contract to a tube or string if a linearly increasing potential is to prevail. This string is stretched by the wake left by the quarks, and it prevents them from moving apart to any macroscopic distance.

In contrast, for the Coulomb potential

$$E(R) = \text{const} - \frac{g_0^2}{4\pi R} \frac{N_c^2 - 1}{2N_c} \tag{1.51}$$

the field around a quark would be spherically symmetric, and the loop average would have the behavior

$$W(C) \xrightarrow[\text{large } C]{} e^{-\text{const perimeter } (C)}. \tag{1.52}$$

This behavior of the loop average is called the "perimeter law." In each order of perturbation theory, it is the perimeter law (1.52), and not the area law (1.49), that holds for the loop average. This simplified interpretation of Wilson's quark confinement criterion can then be stated as follows: The area law corresponds to a potential which increases linearly with the distance and which results in quark confinement, while the perimeter law corresponds to a potential which is incapable of confining quarks.

g) The ratio $\chi(I, J)$

It is difficult to extract information on the nature of the interaction between static quarks in the continuum limit from lattice loop averages because it is necessary to single out an (infinite) factor associated with the renormalization of the quark mass. This factor is an exponential function of the perimeter. Creutz[19] has suggested an elegant method for circumventing this difficulty.

We consider the quantity

$$\chi(I, J) = -\ln \frac{W(I, J)\, W(I-1, J-1)}{W(I-1, J)\, W(I, J-1)}, \tag{1.53}$$

where $W(I,J)$ is the loop average of a rectangle of dimensions $I \times J$. Since the perimeter is

$$(I \times J) = 2I + 2J, \tag{1.54}$$

the factor proportional to the exponential function of the perimeter in $W(I,J)$ cancels out in ratio (1.53) and does not prevent us from taking the continuum limit.

To bring out the physical meaning of χ we again consider a loop in the form of a rectangle stretched out along the "time" axis (Fig. 7). Substitution of the asymptotic behavior (1.46) into definition (1.53) gives us

$$\chi(R, T) \xrightarrow[T\to\infty]{} a\,[E_0(R) - E_0(R-a)]. \tag{1.55}$$

The contribution to $E_0(R)$ from the renormalization of the quark mass cancels out on the right side of Eq. (1.55) (for arbitrary R and T, as we have already seen), and in the continuum limit, $a\to 0$, the difference converts into a derivative of the potential:

$$\chi = a^2 \frac{dE(R)}{dR}. \tag{1.56}$$

In other words, the difference is proportional to the force which the quark and antiquark exert on each other.

The quantity $\chi(I,J)$ has one more useful property. In the limit $a\to 0$ in addition to the linear divergence associated with the renormalization of the quark mass, we have $\ln W(I, J)$, a logarithmic divergence, which stems from the bremsstrahlung of a charged particle upon a change in the direction of its velocity. For a rectangular loop with four corners this divergence can be calculated from the general expression first derived in Ref. 20; the result is

$$[\Delta \ln W]_{\text{brem}} = \frac{g_0^2 (N_c^2-1)}{4\pi^2 N_c} \ln \frac{\text{perimeter}}{a}. \tag{1.57}$$

The bremsstrahlung divergence also cancels out in $\chi(I, J)$ [since the numbers of corners for the loops in the numerator and denominator of the ratio on the right side of (1.53) are identical], and this divergence does not prevent us from taking the continuum limit.

Furthermore, it follows from general theorems regarding the renormalizability of loop averages, proved in Ref. 20, that all the divergences in χ vanish after we make the transition from the "seed" charge g_0^2 to the renormalized charge g_R^2.

Along with these properties, χ has yet another property which makes it convenient for calculating the string tension in the continuum limit. At large values of I and J the substitution of the area law (1.49) into definition (1.53) gives us

$$\chi(I, J) \xrightarrow[\text{large } I, J]{} a^2 K, \tag{1.58}$$

which is independent of the dimensions of the contour. In practice, in Monte Carlo calculations it is the absence of a dependence of this type which tells us when the area law has set in. The results of specific calculations of χ by the Monte Carlo method will be discussed in Section 4.

2. THE MONTE CARLO METHOD

The Monte Carlo method is the best-developed numerical method presently used in lattice theories. It is used widely in various problems in statistical physics. The idea of using the Monte Carlo method to study lattice gauge theories can be credited to Wilson.[21] Jacobs, Creutz, and Rebbi[22,23] worked out a Monte Carlo calculation method for lattice gauge theories.

a) A Monte Carlo algorithm as a Markov process

The Monte Carlo method is used to calculate the functional integrals of Subsection 1d for arbitrary values of the coupling constant. Here we would like to avoid integrating over the matrices U_l at each link l in succession; it is more convenient to replace the multiple integral by a sum over the states of the system and to calculate this sum immediately by the Monte Carlo method.

Let us assume that all the links of a lattice of finite size are numbered. Then some state of the system, which we denote by C, can be characterized by the value of the matrix U_1 at the first link, by the value of U_2 at the second, etc.:

$$C = \{U_1, U_2, \ldots, U_{N_l}\}. \tag{2.1}$$

For simplicity we also assume that the matrices U take on a discrete set of values. It is clear that a sequential summation (or integration) over U can be written as a sum over all states of the system,

$$\sum_{U_1}\sum_{U_2}\cdots\sum_{U_{N_l}} = \sum_{\{U_1, U_2, \ldots, U_{N_l}\}}, \tag{2.2}$$

since a repeated integral is equal to a multidimensional integral for a converging integral of finite multiplicity.

The average (1.32) can then be calculated from

$$\langle Q\rangle = \frac{\sum_C Q(C)\, e^{-\beta S(C)}}{\sum_C e^{-\beta S(C)}}, \tag{2.3}$$

where $Q(C)$ and $S(C)$ are the value of Q (the quantity being averaged) and of the action S in the given state C.

If the total number of states of the system is large (as it is in the case in which we are interested), then we cannot consider each of them, and we use the standard Monte Carlo method to evaluate the sum (2.3).

For this purpose, a sequence of states of the system

$$A = (C_0, C_1, \ldots, C_N) \tag{2.4}$$

is generated in a random manner. If a state C_n appears in sequence (2.4) with a probability $P(C_n)$, then the sum (2.3) can be approximated by

$$\langle Q\rangle \approx \frac{\sum_{n=1}^{N} Q(C_n)\, P^{-1}(C_n)\, e^{-\beta S(C_n)}}{\sum_{n=1}^{N} P^{-1}(C_n)\, e^{-\beta S(C_n)}}. \tag{2.5}$$

Clearly, if β does not tend toward zero in a calculation using (2.5) we would not want all the states in the sequence (2.4) to be equiprobable, since in this case the majority of the configurations would be exponentially suppressed by a Boltzmann factor. It is better to generate the states C_n with a Boltzmann probability

$$P(C_n) \propto e^{-\beta S(C_n)}, \tag{2.6}$$

in order to cancel out this factor. Expression (2.5) then takes the form of an arithmetic mean:

$$\langle Q\rangle \approx \frac{1}{N}\sum_{n=1}^{N} Q(C_n). \tag{2.7}$$

A sequence of states generated with a probability (2.6) is called an "equilibrium sequence of states." The analogy with statistical physics is obvious.

Actually, it is not all that simple to construct an algorithm which generates an equilibrium ensemble of states since the value of the Boltzmann probability is not known at the outset. Here we establish a Markov process, by means of which each new state in sequence (2.4) is constructed from the preceding state. We recall that a "Markov process" is a random process which is completely determined by the probability $W(C\to C')$ for a transition from state C to state C'. This probability does not depend on the history of the system. The transition probability $W(C\to C')$ is chosen in such a way that Boltzmann distribution (2.6) arises in the limit. Here it is sufficient that the transition probability $W(C\to C')$ satisfy the principle of detailed balance:

$$e^{-\beta S(C)} W(C\to C') = e^{-\beta S(C')} W(C'\to C). \tag{2.8}$$

Condition (2.8) is a sufficient condition to ensure, first, that an equilibrium sequence of states will be changed into another equilibrium sequence and, second, that a nonequilibrium sequence will approach an equilibrium sequence as we move through the Markov chain.

The various specific algorithms used for Monte Carlo calculations differ in the choice of transition probability $W(C\to C')$, but property (2.8) holds in all cases. The rate of the convergence to equilibrium differs from one algorithm to another. Some specific algorithms are discussed in the two following subsections.

b) The heat bath method

The functional integral (1.26) which is calculated in the Monte Carlo method looks like the partition function of some (four-dimensional) system with a temperature $1/\beta$. This analogy is the basis for an intuitively clear Monte Carlo algorithm in which a new state C_{n+1} in sequence (2.4) is constructed from the preceding state C_n. This algorithm is the subject of the present subsection.

Each state C is characterized by the values of the matrices on all the links of the lattice [see (2.1)], and the current values of these matrices are stored in the computer memory. The initial state

$$C_0 = \{U_1^{(0)}, U_2^{(0)}, \ldots, U_{N_l}^{(0)}\} \tag{2.9}$$

is constructed "manually." For example, it might be assumed for definiteness that the system is completely ordered in its initial state, i.e., that the matrices $U^{(0)}$ are unit matrices on all the links. If the temperature $1/\beta$ is not too low, this ordered state of the system is a long way from the states typical of the given temperature. It is clear from the analogy with a partition function that the system can be brought to an equilibrium state by applying a reservoir heated to a temperature $1/\beta$ to each link of the lattice in succession. A Monte Carlo algorithm which simulates this physical process is the "heat bath method."[24]

Let us examine in more detail how the computer "applies the reservoir" to the links. We assume that some initial state (2.9) is given. We construct a new state in the following way: On the first link we replace the old matrix $U_1^{(0)}$ by the new one $U_1^{(1)}$, which is chosen at random from the entire gauge group with the probability proportional to a Boltzmann factor,

$$W_1(U_1^0 \to U_1^{(1)}) \propto e^{-\beta S(U_1^{(1)})}. \tag{2.10}$$

The action is calculated for the new configuration

$$\{U_1^{(1)}, U_2^{(0)}, \ldots, U_{N_l}^{(0)}\}, \tag{2.11}$$

in which the new value $U_1^{(1)}$ corresponds to the first link, while the old values correspond to the other links. Once the new value of the matrix U_1 has been chosen, it is stored in that cell of the computer memory which previously held the old value, $U_1^{(0)}$, which is "forgotten." We have thus "applied the reservoir" to the first link of the lattice, and as a result the system has gone from state (2.9) to state (2.11).

The same procedure is then applied in succession to the second, third, and all other links of the lattice. In each step the probability with which the new element is chosen is proportional to a Boltzmann factor:

$$W_M(U_M^{(0)} \to U_M^{(1)}) = \text{const}\cdot e^{-\beta S(U_M^{(1)})}, \tag{2.12}$$

where the action is calculated for the configuration in which the values of the matrices U on all the links except that currently under consideration are fixed at their current values; only U_M changes. The application of this procedure to all the links of the lattice constitutes one Monte Carlo "sweep" or "iteration." The transition probability $W(C\to C')$ is thus given by

$$W(C\to C') = \prod_{M=1}^{N_l} W_M(U_M \to U'_M), \tag{2.13}$$

where the product is over all the links of the lattice.

The old value of the matrix U on a given link, we might note, is not directly involved in the procedure for generating a new element. Nevertheless, since the old element was, generally speaking, correlated with the values of the matrix U on the neighboring links, it does have an indirect effect on the choice of the new element. The probability (2.12) is directly determined by the values of the matrices U on those neighboring links which, along with the link presently under con-

sideration, form the boundary of some plaquette. The number of such neighboring links for action (1.18) is 18; these links, along with the link under consideration, form $2(d-1)=6$ plaquettes which border the given link. In the heat bath method, therefore, it is actually sufficient to consider only these six plaquettes in each Monte Carlo step.

Because of the correlation which we just mentioned, a single sweep will generally not be enough to bring the system to a equilibrium state. It is necessary to sweep through the entire lattice many times in order to "make the system forget its initial state." The analogy between the heat bath method and the physical process suggests that a thermal equilibrium will ultimately be reached and it will be reached in the smallest number of sweeps (the comparison is being made with other methods). However, the heat bath method proposed in Refs. 22 and 23 for studying lattice gauge theories turned out to be effective only for the simplest gauge groups [U(1), SU(2), SU(3), and discrete subgroups]. For more complex groups the generation of new elements by the heat bath method requires an unacceptable amount of computer time, and we instead use the method discussed in the following subsection.

c) The Metropolis method

The Metropolis method,[25] a standard method in statistical physics, is used along with the heat bath method for integrations over gauge fields. Although this method requires more sweeps to bring the system to equilibrium, the calculations at each step are simpler and faster. For gauge groups more complicated than the SU(2) group it is thus frequently possible to save computer time by using the Metropolis method.

As in the heat bath method, the value of only the matrix on one link is changed in each Monte Carlo step in the Metropolis method, so that the probability for a transition from one configuration to another is determined by the product of the transition probabilities at the various links, (2.13). In contrast with the heat bath method, however, the transition probability for the Metropolis method, $W_M(U_M \to U'_M)$, depends explicitly on both the new value U'_M and the old value U_M. In the simplest version of the method the new value U'_M is chosen at random from all the group elements, with a uniform probability (for discrete groups one always chooses $U'_M \neq U_M$). The change in the action upon the replacement of U_M by U'_M is then calculated:

$$\Delta S = S(U'_M) - S(U_M). \tag{2.14}$$

If the action decreases, i.e., if $\Delta S < 0$, upon the replacement of U_M by U'_M, then this new value U'_M is chosen as the value of the matrix U on the given link M, and we can proceed to the next step.

The principle of detailed balance, (2.8), determines the remainder of the algorithm. If the action does not decrease when U_M is replaced by U'_M [i.e., if the value calculated from (2.14) satisfies $\Delta S \geqslant 0$], then a random-number generator is consulted for a random number r with a uniform distribution between 0 and 1. The value of r is then compared with $\exp(-\beta\Delta S)$; if

$$e^{-\beta\Delta S} > r, \tag{2.15}$$

then U_M is replaced by the new value U'_M. If condition (2.15) does not hold, then the matrix U on the given link is left at its old value U_M, and we move on to the next step.

Since for $\Delta S < 0$ we have $\exp(-\beta\Delta S) > 1$, condition (2.15) always holds for $\Delta S < 0$. Consequently, the two parts of the algorithm can conveniently be combined into the single condition that if inequality (2.15) holds then the new value U'_M is assigned, while if this inequality does not hold then the old value U_M is retained.

We might also note that in calculations by the Metropolis method it is necessary to calculate only the change in the action upon the replacement of U_M by U'_M on a single link in each step. As we discussed in the preceding subsection, this quantity is determined by only the values of the matrices U on the links which form the boundaries of the six plaquettes which border the particular link under consideration.

The next Monte Carlo step may consist of the application of the Metropolis method to both another link and the same link. It is frequently beneficial to repeat the Metropolis algorithm several times [10–20 times for the SU(2) group] on the same link before moving on to the next link, since this repetition requires very little computer time in comparison with the search for the neighboring link and the various operations on it. Clearly, if the algorithm is repeated a very large number of times on a given link before the neighboring link is considered then the given link will reach a state of thermodynamic equilibrium with its neighbors. In the case of a very large number of repetitions, therefore, the Metropolis method simulates the heat bath method. In practice, the optimum number of repetitions is determined for each gauge group empirically on the basis of the expenditure of computer time.

Another important saving of computer time is possible if (in the Metropolis method) the proposed new element U'_M is chosen not at random from the entire group in each step but by the following rule: We first construct in a random fashion a table of several group elements, $Q_1, \ldots, Q_K$; this table also includes the reciprocal of each element. We now construct the proposed new element U'_M on each step as the product of the old element U_M and an element Q_i chosen in an arbitrary way from the table:

$$U'_M = Q_i U_M. \tag{2.16}$$

How well the table is constructed goes a long way toward determining how successfully it can be used. In the construction of the table it is better to generate the elements Q near a unit element, rather than distributed uniformly over the entire group. The weight factor is made dependent on β to hasten the convergence.

The Metropolis method with a table is particularly convenient for discrete gauge groups. An important saving in computer time is achieved in this case by using a multiplication table of the elements of the group; this table is specified before the calculations are begun, along with a table of values of characters. The operations of multiplying group elements and calculating traces then become simply logic operations.

This approach can also be taken for a continuum group, by approximating it by a discrete subgroup. It turns out that the SU(2) group can be approximated extremely well over the range of β of interest by a 120-element $\bar{Y}$ icosahedral subgroup.[26–28] Unfortunately, a satisfactory discrete approximation of the SU(3) group requires examining subgroups with very large numbers of elements, for which the multiplication table exceeds the capacity of the computer memory. Consequently, this method cannot be used for the SU(3) group,[29,30] and we are forced to work exclusively with the continuum group itself (but see Ref. 31).

In the Metropolis method, for which the transition probability $W_M(U_M \to U'_M)$ depends explicitly on the old value U_M, successive states of the ensemble, (2.4), are generally correlated. Since the calculation of $Q(C_n)$ for each configuration C_n upon the averaging in (2.7) generally requires far more computer time than a single sweep, we would like to select independent configurations for the averaging. Here it is sufficient to make an appropriate number of "dummy" runs through the lattice between calculations of $Q(C_n)$. The correlation length may be reduced by replacing the regular, prespecified order for circuiting the lattice by a random order, with the link M being chosen at random in each step. A random circuit of the lattice is also used in the heat-bath calculations to reduce the statistical error, for example, in the calculation of glueball masses which is discussed in Section 4 below.

To conclude this section we refer the reader to Refs 32–36 for detailed descriptions of the programs used for Monte Carlo calculations in lattice gauge theories.

3. THE "WHAT" AND "HOW" OF MONTE CARLO CALCULATIONS

Before the Monte Carlo method was adopted for nonperturbative calculations of physical quantities in QCD, it had been developed in simpler calculations. Although the quantities which were calculated and the resulting numbers have no direct bearing on the continuum limit (and thus are frequently called "lattice artifacts"), the results were important in two ways: First, they were compared with the results obtained by other methods (where available), and the reliability of the Monte Carlo method was thereby demonstrated. Second, the lattice artifacts have some qualitative implications for the continuum limit.

The Monte Carlo method was initially used by Jacobs, Creutz, and Rebbi[22,23] to study Abelian lattice gauge theories. The first Monte Carlo calculations for the non-Abelian gauge groups SU(2) and SU(3) were carried out by Creutz[37,38,19] and Wilson.[39] The phase structure of lattice group theories with other non-Abelian groups has been studied in Refs. 40–47.

a) Specific energy: the gauge groups SU(2) and SU(3)

The simplest quantity calculated by the Monte Carlo method is the specific energy

$$E = \left\langle 1 - \frac{1}{N_c} \operatorname{tr} U_p \right\rangle, \tag{3.1}$$

where the average is understood in the sense of the functional integral (1.32). The term "specific energy" stems from the analogy with the statistical system, which we discussed earlier. Since the quantity in (3.1) is identical for all plaquettes in the absence of an external field, E is the same as the average value of the action per plaquette:

$$E = \frac{1}{N_p} \langle S \rangle, \tag{3.2}$$

where the number of plaquettes is determined by (1.5). Relation (3.2) may be rewritten as the familiar relationship between the specific energy and the partition function (1.26):

$$E(\beta) = -\frac{1}{N_p} \frac{\partial}{\partial \beta} \ln Z(\beta). \tag{3.3}$$

Equation (3.2) is used to calculate the specific energy by the Monte Carlo method. The equilibrium ensemble of states (2.4) is generated by one of the algorithms discussed in Section 2. For each state one calculates

$$E_n = \frac{1}{N_p} S(C_n), \tag{3.4}$$

which has the meaning of the energy density in the given state. An average is then calculated from general expression (2.7).

The first problem which must be solved is to choose the initial state. A good choice is a state close to some typical state for the given temperature. Clearly, in the limit $\beta \to \infty$ (or, for the temperature, $\beta^{-1} \to 0$), the matrices $U_{x,\mu}$ are "frozen" near some value, so that we have

$$E(\beta) \xrightarrow[\beta \to \infty]{} 0. \tag{3.5}$$

At large values of β one accordingly chooses an "ordered" initial state ($U_{x,\mu} = 1$ on all links of the lattice). In the opposite limit $\beta \to 0$ (or, for the temperature $\beta^{-1} \to \infty$), the matrices $U_{x,\mu}$ fluctuate over the entire group, so that we have

$$E(\beta) \xrightarrow[\beta \to 0]{} 1 \tag{3.6}$$

[compare with the explicit expression (1.39) for $W(\partial p) = 1 - E$]. At small values of β one accordingly selects a "random" initial state (the $U_{x,\mu}$ on each link are chosen at random, from a uniform distribution over the group).

Completely ordered and completely random states can be used as initial states for intermediate values of β. In this case, however, several sweeps will be required to bring the system to thermodynamic equilibrium. Figure 8, taken from the original paper by Creutz,[38] shows results calculated for E_n for the SU(2) gauge group as a function of n—the number of sweeps. These calculations were carried out for lattices of various dimensions with $\beta = 2.3$ by the heat bath method. The upper values correspond to a random initial state, and the lower values to an ordered initial state. We see from Fig. 8 that both a superheated system (a random start) and a supercooled system (an ordered start) reach thermodynamic equilibrium in only 20–30 sweeps, so that the values of E_n stabilize near certain values around which thermal fluctuations subsequently occur. These fluctuations are significant for a lattice of size 4^4 and essentially indistinguishable for a lattice of size 10^4. The reason is that in the calculations from (3.4) a spatial average is taken for each configuration, so that the fluctuations are greatly reduced.

The specific energy can be calculated more accurately

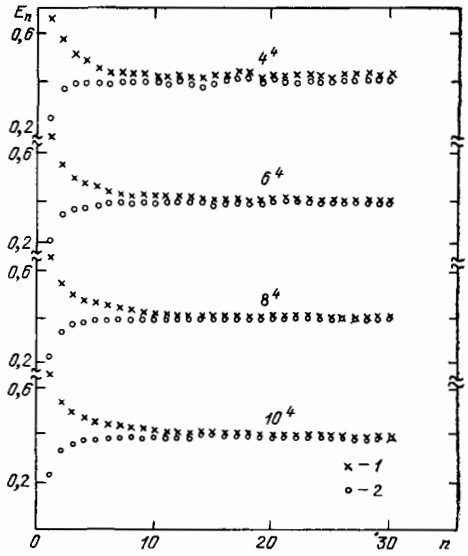

FIG. 8. E_n as a function of the number of sweeps according to calculations from expression (3.4) for a lattice theory with the SU(2) gauge group with $\beta = 2.3$ on lattices of various sizes. 1—Random initial state (Subsection 3a); 2—ordered initial state (this figure is taken from the paper[38] by Creutz).

by averaging E_n over several configurations. Clearly, we would like to exclude from the average those configurations for which equilibrium has not yet been reached. Correspondingly, the first few configurations, say 20 in Fig. 8, are discarded, and the average is carried over the remaining ten. Actually, there are limitless possibilities for improving this average value, since a CDC-7600 computer can perform, say, 20 000 sweeps in an extremely short time.

The number of sweeps is frequently identified with the time for the analogous statistical system, so that an average over configurations is none other than an average over time in statistical physics. Accordingly, in our case the number 20 is, in arbitrary units, the length of time over which the superheated or supercooled system must interact with the reservoir in order to reach equilibrium at the given temperature. Since the number of sweeps is proportional to the actual computer time, the statistical errors fall off as the square

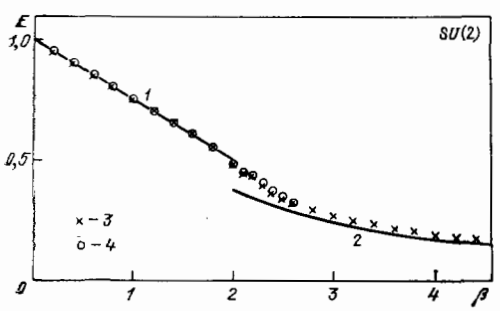

FIG. 9. The specific energy E as a function of the coupling constant β in the SU(2) theory according to expression (3.1). 1, 2—Lower order of the strong-coupling and weak-coupling expansions, respectively, described by $E = 1 - \beta/4$ and $E = 3\beta/4$ [see (1.39b) and (3.13)]; 3— heating; 4—cooling (Subsection 3a) (this figure is from the paper[37] by Creutz).

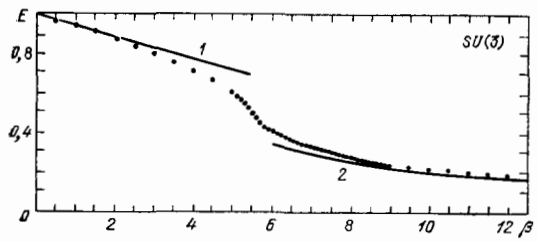

FIG. 10. The same as in Fig. 9, but for the SU(3) gauge theory (this figure is from the paper[48] by Creutz and Moriarty).

root of the computer time in Monte Carlo calculations.

The first step in a Monte Carlo study of lattice gauge theories is to calculate the specific energy as a function of β. The energy $E(\beta)$ is calculated for a finite number of values of β. It turns out to be a poor choice to start with an ordered or random configuration each time. It is better to heat (or cool) the system in small steps along β, using as an initial state in each step a configuration from the equilibrium ensemble in the preceding step. Since the temperature change is small, equilibrium is reached rapidly.

Figure 9 shows the results of some corresponding calculations of $E(\beta)$ (also called the "thermal cycle"), from the first paper by Creutz[37] on a 5^4 lattice. The crosses correspond to a heating of the system and the circles to a cooling. Several "dummy" sweeps were carried out at each point, and then an average is taken over an equilibrium ensemble of six configurations. The total number of sweeps at each point was about 20 during heating and an equal number during cooling. The heating process was begun with an ordered configuration, and the cooling with a random configuration.

From Fig. 9 we see that $E(\beta)$ is a smooth function, so that no phase transition occurs with increasing β in the SU(2) lattice gauge theory. The function $E(\beta)$ for the SU(3) gauge group, shown in Fig. 10, is similar in form.[48]

b) The case of a phase transition: the gauge groups Z_N

The SU(2) and SU(3) gauge groups examined in the preceding subsection are special cases in the sense that for them $E(\beta)$ is a smooth function, and no phase transition occurs as β is varied. The Monte Carlo method has also proved useful for studying systems which do exhibit a phase transition, in particular, lattice gauge theories with Abelian groups. The simplest Abelian group is the Z_N group, whose elements are the N-th order roots of -1 [$U_{x,\mu} = \exp(2\pi i n/N)$, $n = 0, \ldots, N-1$], and group multiplication is defined as the ordinary multiplication of complex numbers. Since the elements of Z_N are numbers, rather than matrices, we can omit the trace sign from all the equations and set $N_c = 1$ (N_c is always equal to the trace of the unit element). Definition (3.1), for example, becomes

$$E = \langle (1 - U_p) \rangle. \tag{3.7}$$

An integration over the invariant measure for the Z_N group reduces to a summation over N group elements:

$$\int_{Z_N} dU_{x,\mu} = \frac{1}{N} \sum_{U_{x,\mu} = e^{2\pi i n/N}}. \tag{3.8}$$

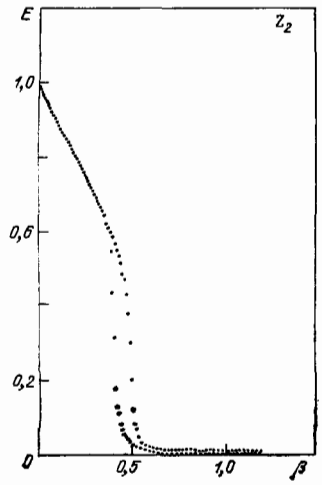

FIG. 11. The same as in Fig. 9, but for the Z_2 gauge group. In the hysteresis region the lower points correspond to heating and the upper points to cooling (Subsection 3b) (this figure is from the paper[23] by Jacobs, Creutz, and Rebbi).

The Monte Carlo method is used to find the point of the phase transition and to determine its nature (first- or second-order). Although this might seem strange since no phase transition occurs for a system with a finite number of degrees of freedom (such as a Z_N theory on a lattice of finite size), the number of degrees of freedom for the lattices of interest is so large (but finite) that the behavior of the system is indistinguishable from a phase transition (especially for a first-order transition, where the specific energy has a discontinuity).

To find the point of the phase transition we first construct a thermal cycle as described in Subsection 3a. Since the system must draw much heat from the reservoir at the point of a first-order phase transition, the duration of the interaction with the reservoir must be long if equilibrium is to be reached. In other words, if fewer sweeps than are necessary to reach equilibrium are carried out near the phase transition, the system will remain supercooled as it is being heated (or superheated as it is being cooled), and the thermal cycle will exhibit a characteristic hysteresis. Figure 11, from Ref. 23, shows a thermal cycle for the Z_2 gauge group. A hysteresis is observed near the point $\beta = 0.45$. If the number of sweeps is increased, the hysteresis vanishes, and we are left with simply an abrupt change (more abrupt, the greater the size of the lattice) in the behavior of $E(\beta)$ near the phase transition. Figure 12 shows the results of these calculations[49] for the Z_2 gauge group.

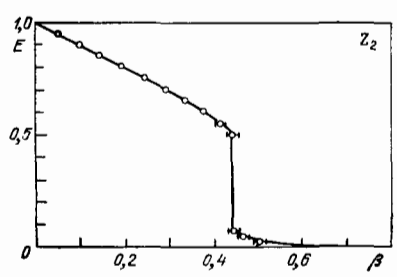

FIG. 12. The same as in Fig. 11, but with more sweeps.[49]

By itself a hysteresis does not mean that a first-order phase transition occurs in this region. A hysteresis is observed whenever the period required to reach equilibrium increases at some β, and the number of sweeps is smaller than this period. Therefore, a hysteresis (although not as pronounced) can be observed near a second-order phase transition, where the period required to reach equilibrium also increases. Furthermore, even for the SU(2) gauge group, which exhibits no phase transition at all, the period required to reach equilibrium increases slightly near the point $\beta = 2.2$, and a hysteresis is observed if the number of sweeps is too small (5–10).

There is a way to determine the order of a phase transition at a hysteresis point (if a transition occurs at all). We hold β equal to the position of the center of the hysteresis loop and construct for this value of β a curve similar to that in Fig. 8, carrying out far more sweeps than are necessary to reach equilibrium. If, at the given value of β, a first-order phase transition occurs, then we go into two phases, which differ in specific energy, depending on the initial state. For a second-order phase transition, the specific energies of the two phases are instead identical.

Figure 13, a and b, also shows some results[23] for the Z_2 gauge group (a first-order phase transition) and the Z_6 gauge group (second-order). The values of E_n were calculated after each ten sweeps. From Fig. 13a we see that the system rapidly goes into one of two phases and then remains stable over many sweeps. Actually, one of these phases is metastable at

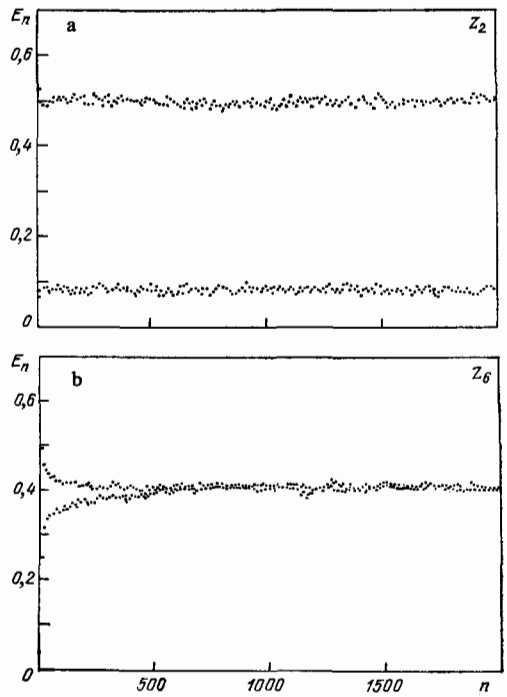

FIG. 13. E_n as a function of the number of sweeps according to calculations from expression (3.4) for the value of the coupling constant near the center of the hysteresis loop. a—The Z_2 gauge group (first-order phase transition); b—the Z_6 gauge group (second-order phase transition). The upper (lower) points correspond to a random (ordered) initial state (Subsection 3a) (this figure is taken from the paper[23] by Jacobs, Creutz and Rebbi).

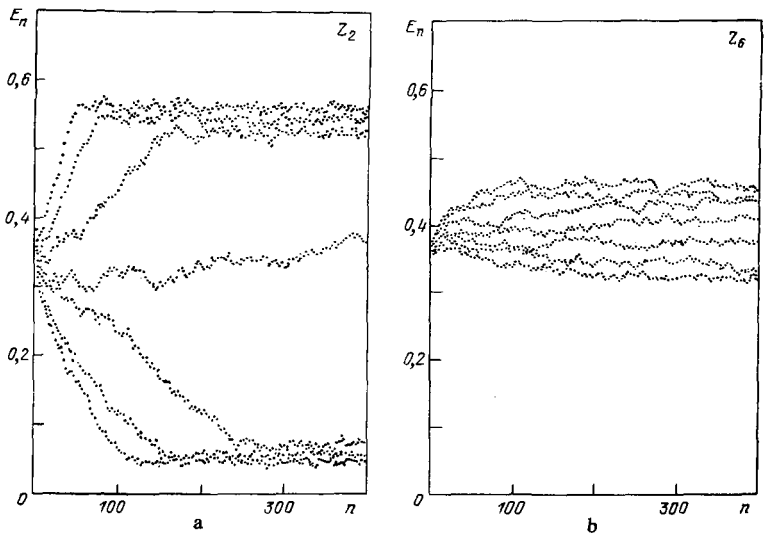

FIG. 14. The same as in Fig. 13, but for a mixed initial state and various values of the coupling constant from near the center of the hysteresis loop[23] (Subsection 3b).

the given value of β (since we cannot reach the transition point exactly), and the system ultimately leaves this phase and goes into a stable phase. The transition occurs over an extremely small number of sweeps (in comparison with the "lifetime" of the metastable phase) and usually serves as one more piece of evidence for a first-order phase transition. In contrast, in Fig. 13b we see a convergence (rather slow) to the same value of the specific energy.

In working from the position of the center of the hysteresis loop we can find only an approximation of that value of β (which we denote by β_c) at which the transition occurs. The value of β_c can be found more accurately by the following approach.[23] As the initial state we use a "mixed" state for which the $U_{x,\mu}$ on half of the links of the lattice are chosen equal to the unit element, while those on the other half are chosen at random. The evolution of this state over time (with increasing number of sweeps) is studied for several closely spaced values of β from near the center of the hysteresis loop. Figure 14, a and b, shows some corresponding results[23] for the Z_2 and Z_6 gauge groups. Figure 14a is typical of a first-order phase transition, with the system rapidly entering a state for which the stable phase fills the entire lattice. If β is very close to β_c, however, the relaxation period increases dramatically, and two phases coexist over a large number of sweeps, so that the values of E_n remain approximately equal to the initial value. This property is exploited for an accurate determination of β_c. For a second-order transition, in contrast, the relaxation period depends only weakly on β (Fig. 14b).

c) Phase structure of Abelian gauge groups. Compact electrodynamics

The procedure of Jacobs, Creutz, and Rebbi[23] described above has been used for Monte Carlo studies of Abelian lattice gauge theories with the Z_N groups and the group U(1) ("compact electrodynamics"), which is the limit of the Z_N group as $N\to\infty$. Figure 15, from 23, shows the coupling constants at which phase transitions occur. For the Z_2, Z_3, and Z_4 gauge groups with $\beta > 0$ only a single phase transition, of first order, occurs. For the Z_N groups with $N\geqslant 5$ there are instead two second-order phase transitions. The transition points separate three phases with the following properties: I) a confinement phase; II) an intermediate phase; III) a Higgs phase.

The area law (1.49) holds for the loop averages in the confinement phase, while the perimeter law (1.52) holds in the intermediate and Higgs phases. In order to distinguish the intermediate phase from the Higgs phase we need a finer criterion than a simple calculation of the loop average. Physically, the difference between these two phases is that in the intermediate phase there are massless excitations—photons—which lead to long-range forces of the Coulomb type. In the Higgs phase the photon is massive, and there are only Yukawa forces, which fall off rapidly with distance. The reason for the existence of a Higgs phase for the discrete groups

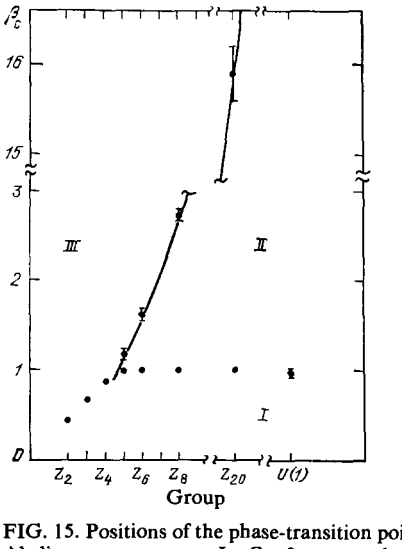

FIG. 15. Positions of the phase-transition points for lattice theories with Abelian gauge groups. I—Confinement phase; II—intermediate (Coulomb) phase; III—Higgs phase (Subsection 3c). The solid curve is plotted from Eqs. (3.9) and (3.10) (this figure is from the paper[23] by Jacobs, Creutz, and Rebbi).

Z_N is that the excitation spectrum is separated from the ground state by an "energy gap"

$$\Delta S = 1 - \cos\frac{2\pi}{N}. \tag{3.9}$$

Monte Carlo calculations have yielded[23]

$$\beta_c' = \frac{0{,}78}{\Delta S} \tag{3.10}$$

for the phase transition between the Coulomb and Higgs phase; i.e., the critical "temperature" is proportional to the size of the energy gap.

According to Eqs. (3.9) and (3.10) we have $\beta_c' \sim N^2$ in the limit $N \to \infty$, so that in the U(1) limit we are left with only two phases: the confinement and intermediate phases. A study of the phase transition which separates these two phases by the method outlined above does not tell us whether it is actually a second-order (and not higher-order) phase transition which occurs. This point can be resolved by studying the "specific heat,"

$$C(\beta) = -\beta^2 \frac{dE(\beta)}{d\beta}, \tag{3.11}$$

which is equal to the derivative of the specific energy with respect to the temperature $1/\beta$. The specific heat becomes infinite at the point of a second-order phase transition.

Calculations of the specific heat for the U(1) lattice gauge theory carried out by Lautrup and Nauenberg[50] (see also Refs. 51 and 52) indicate a second-order phase transition. Since a phase transition cannot occur on a lattice of finite size, so that the specific heat cannot become infinite, the calculations were carried out on lattices of sizes 4^4, 5^4, and 6^4, and then the results were extrapolated to an infinite lattice. The extrapolation yielded the following value[50] for β_c:

$$\beta_c = 1.005. \tag{3.12}$$

The existence of a second-order phase transition in compact lattice electrodynamics (more precisely, photodynamics, since the polarization of the vacuum by electrons is ignored) is important for taking the continuum limit. If the constant β is chosen near β_c then the correlation length will be large (infiite at a second-order phase transition), and the continuum limit will be reached. If $\beta < \beta_c$, we find a theory with confined electrons, while at $\beta > \beta_c$ there is no electron confinement. Fortunately, the charge of the electron in our world is small, so that the situation which prevails is $\beta > \beta_c$, with unconfined electrons.

In the U(1) lattice gauge theory the confinement at small values of β occurs for the same reason as in the non-Abelian case: because of the property of compactness of the gauge group, which leads to orthogonality relation (1.36). As discussed in Subsection 1d the compactness in the limit $a \to 0$ stems from the circumstance that the discontinuities of the vector potential of magnitude $\approx 2\pi/a$ are not accompanied by changes in the action. In the U(1) lattice gauge theory this property prevails only at $\beta < \beta_c$; at $\beta > \beta_c$ the compactness is disrupted, and we are dealing with an ordinary noncompact electrodynamics.

To conclude this subsection we note that the phase structure of Abelian lattice gauge theories was predicted in Refs. 14, 53, and 54 for the Z_N gauge groups and in Refs. 55 for the U(1) gauge group before they were studied by the Monte Carlo method. However, the Monte Carlo calculations have established that three phases appear, beginning at $N = 5$, and—the most important—they have established the order of these transitions.

d) Lattice artifacts. The gauge groups SU(N) and U(N)

As mentioned in Subsection 3a, $E(\beta)$ is a smooth function for the SU(2) gauge group (Fig. 9). At $\beta < 2$ the Monte Carlo data are described by the strong-coupling expansion [the straight line in Fig. 9 is drawn from Eq. (1.39b) for $1 - E$]. At large values of β, the function $E(\beta)$ can be found as a series in $1/\beta$ (the "weak-coupling expansion"), through a calculation of functional integrals by the method of steepest descent. The first approximation of $E(\beta)$ is

$$E(\beta) = \frac{n}{d\beta} + O(\beta^{-2}), \tag{3.13}$$

where n is the number of generators of the gauge group [$n = N^2 - 1$ for the SU(N) group, and $n = N^2$ for the U(N) group], and $d = 4$ is the dimensionality of the space. Figure 9 also shows a line drawn from Eq. (3.13); it describes the Monte Carlo data at $\beta > 3$.

By taking into account the next few terms in the strong- and weak-coupling expansions we can describe the Monte Carlo data on $E(\beta)$ everywhere except near the point $\beta = 2.2$, where we see (Fig. 9) the sharpest change in the behavior of the function $E(\beta)$. This vicinity is the "crossover region" between the regions of strong and weak coupling. The reader is referred to Refs. 56 regarding the possibility of describing the function $E(\beta)$ in the crossover region.

To determine whether a second-order phase transition occurs at the point $\beta = 2.2$, Lautrup and Nauenberg[57] calculated the specific heat (3.11) by the Monte Carlo method for lattices of sizes 4^4, 5^4, and 6^4. These calculations revealed that the specific heat has a clearly defined peak at $\beta = 2.2$, whose height [in contrast with that in the U(1) lattice gauge theory] does not increase substantially as the size of the lattice is increased. An extrapolation to an infinite lattice carried out in Ref. 58 on the basis of the scaling laws on a lattice of finite size revealed that the specific heat remains finite in the limit of an infinite lattice. Consequently, a second-order phase transition does not occur at $\beta \approx 2.2$ in the SU(2) lattice gauge theory; there is simply a peak in this specific heat.

Analogously, in the case of the SU(3) gauge group there is a crossover region between regions of strong and weak coupling, and there is a peak in the specific heat at $\beta \approx 5.5$ (Ref. 48).

For the SU(N) gauge groups with $N \geqslant 4$, however, the regions in which the strong- and weak-coupling expansions are valid are separated by a first-order phase transition. This fact was established by the Monte Carlo method in Refs. 40 and 41 for $N = 4$, 5, and 6. A similar phase transition has been found[42] for the U(N) gauge groups with $N = 2$–6. The values found for the constant β_c at which these phase transitions occur are listed in Table I along with the values of β_c correpsonding to the peak in the specific heat for the SU(2)

TABLE I. Positions of the phase transitions (the peaks in the specific heat) for lattice theories with the SU(N) (Refs. 37, 40, 41, 48, and 57) and U(N) (Ref. 42) gauge groups.

	N	2	3	4	5	6
SU(N)	β_c/N^2	0,56	0,61	0,64	0,66	0,67±0,03
U(N)	β_c/N^2	0,83±0,01	0,784±0,001	0,76±0,04	0,75±0,04	0,76±0,07

and SU(3) gauge groups. We see that the quantity β_c/N^2 depends only weakly on N, so that the limit of large N [which is identical for the SU(N) and U(N) gauge groups] is reached quite soon. The Monte Carlo method has been used to calculate β_c/N^2 in the limit $N\to\infty$ by making use of the equivalence of a gauge theory on an infinite lattice to the Eguchi-Kawai model[59] on a 1^4 lattice. The resulting value,[50,61]

$$\frac{\beta_c}{N^2}=0.66\pm 0.02 \quad \text{as} \quad N\to\infty \tag{3.14}$$

agrees with the data shown in Table I.

The occurrence of a first-order phase transition at large N in lattice gauge theories with U(N) groups [and thus SU(N) groups] was predicted by Green and Samuel.[62] The value in (3.14) agrees with the value found by Green and Samuel by analytic calculations. We might add that the values found for β_c in the SU(N) and U(N) lattice gauge theories are in excellent agreement with the results calculated by the mean-field method.[63,64]

e) Mixed action. Nature of the peak in the specific heat

The action (1.18) is the simplest action of a lattice gauge theory which is compatible with the requirement of local gauge invariance and which also has the correct naive local limit. From the mathematical standpoint, the quantity $\mathrm{tr}U_p$ is the character in the fundamental representation of a gauge group. The next step up the complexity scale is the character in the associated representation which is related to $\mathrm{tr}U_p$ by

$$\chi_A(U_p)=|\ \mathrm{tr}\ U_p\ |^2-1. \tag{3.15}$$

The simplest modification of the Wilson action (1.18) contains a sum of two terms[40,65]:

$$S^{\mathrm{mix}}=\sum_p\left[\beta\left(1-\frac{1}{N}\,\mathrm{Re}\,\mathrm{tr}\,U_p\right)+\beta_A\left(1-\frac{1}{N^2}\,|\mathrm{tr}\,U_p|^2\right)\right]. \tag{3.16}$$

This action has a second-order gauge invariance and also has the correct naive local limit. The charge g_0 is related to β and β_A by

$$g_0^2=\frac{2N}{\beta+2\beta_A} \tag{3.17}$$

[cf. (1.33) for the Wilson action].

The action (3.16) has been named the "mixed action." A study of a lattice gauge theory with the action (3.16) has revealed some extremely useful information about the types of fluctuations of the dynamic variable $U_{x,\mu}$ which exist at a given value of β. This study has also revealed the nature of the peak in the specific heat of SU(2) and SU(3) lattice gauge theories with a Wilson action. Furthermore, the physical results should not depend on the choice of lattice action, so that by using the action (3.16) one can determine which of the results which have been obtained are unrelated to the lattice regularization and are pertinent to the continuum theory.

In the limit $\beta_A\to 0$ the action (3.16) converts into the action (1.18). In the limit $\beta_A\to\infty$, only discrete fluctuations of the matrix $U_{x,\mu}$, of the form

$$U_{x,\mu}=e^{2\pi i n_{x,\mu}/N}I, \qquad n_{x,\mu}=0,\ \ldots,\ N-1, \tag{3.18}$$

survive. These are elements of the group Z_N, the "center of the SU(N) gauge group." Fluctuations of this sort leave the second term in action (3.16) invariant and thus are extremal in the limit $\beta_A\to\infty$. In the limit $\beta_A\to\infty$ we therefore find a Z_N lattice gauge theory (with a constant β). In the opposite limit $\beta\to 0$ we find a lattice gauge theory with the SU(N)/Z_N group, since at $\beta=0$ the action (3.16) is insensitive to transformations of the matrix $U_{x,\mu}$ to an element of the group center.

The phase structure of lattice gauge theories with the SU(N) and Z_N groups was studied above. An analogous study of the phase structure of the SU(N)/Z_N lattice gauge group by the Monte Carlo method was carried out in Refs. 43 and 44 for $N=2$ and in Ref. 45 for $N=3$–6 (see also Refs. 46, 30, and 47), where it was shown that a single first-order phase transition occurs in these theories.

Let us take a more detailed look at the simple case $N=2$. We know that the SU(2)/Z_2 group coincides with the SO(3) rotation group. Lattice gauge theories with the SU(2) and SO(3) groups have identical weak-coupling decompositions and should therefore coincide at small values of g_0^2. However, the strong-coupling expansions, which are sensitive to the global properties of the gauge group, are completely dissimilar. Monte Carlo calculations have shown[43,44] that with increasing β_A in the SO(3) lattice gauge theory a phase transition occurs, after which the theory is essentially identical to the lattice gauge theory with the SU(2) group. The nature of the fluctuations of the gauge field, which is "frozen" at the transition point, is described below.

The phase diagram of the mixed SU(2)–SO(3) lattice gauge theory determined by the action (3.16) was first derived by Bhanot and Creutz.[46] This diagram is shown in Fig. 16. The phase transition in the limit $\beta_A\to\infty$ corresponds to the Z_2 theory, and that in the limit $\beta\to 0$ corresponds to the SO(3) theory. The lines of these phase transitions continue through the β,β_A plane, meet at the point B, and then merge,

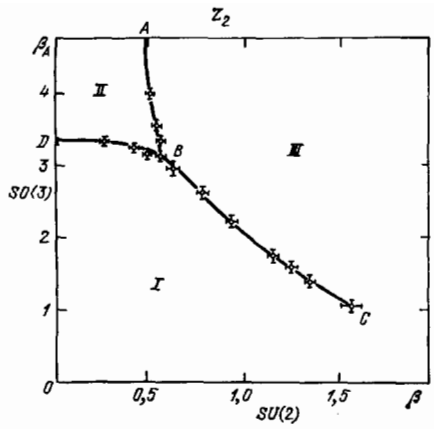

FIG. 16. Phase diagram of a lattice gauge theory with a mixed SU(2)–SO(3) action, (3.16). The Roman numerals label regions with different values of the density of Z_2 vortexes ($\overline{E}$) and Z_2 monopoles ($\overline{M}$) according to calculations from Eqs. (3.22) and (3.23). I—$\overline{E}\approx\overline{M}\approx 0.5$; II—$\overline{E}\approx 0.5$, $\overline{M}\approx 0$; III—$\overline{E}\approx\overline{M}\approx 0$. (This phase diagram was obtained by Bhanot and Creutz.[46])

forming line BC. This line ends at the point C, so that at smaller values of β_A there is no phase transition. If we were to continue the line BC downward, it would intersect the $\beta_A = 0$ axis near the point $\beta = 2.2$, where the SU(2) theory has a crossover region. The peak in the specific heat in the SU(2) lattice gauge theory is therefore generally attributed to the proximity of the critical point on the phase plane of the mixed SU(2)–SO(3) lattice gauge theory.

The phase diagram[30] for $N = 3$ is just like that in Fig. 16. All the phase transitions are of first order; the point C lies above the $\beta_A = 0$ axis; and a continuation of the line BC intersects the $\beta_A = 0$ axis in the crossover region. At $N \geqslant 4$, however, the point C lies below the $\beta_A = 0$ axis, so that the line BC intersects the $\beta_A = 0$ axis in a region where a phase transition occurs in the SU(N) lattice gauge theory. For any finite N the point C lies at a finite value[47] of β_A, so that there are paths on the β, β_A plane which connect the two phases of the SU(N) lattice gauge theory without intersecting phase-transition lines. Consequently, the phase transition observed in the Wilson SU(N) lattice gauge theory at $N \geqslant 4$ is unrelated to deconfinement: It is simply an artifact of the Wilson action. The existence of a region of analyticity on the phase plane of the mixed lattice gauge theory also implies that the free energy is an analytic function of β and β_A, but it is a multivalued function near the phase-transition line.

The occurrence of a first-order phase transition in the SU(N)/Z_N lattice gauge theory and the presence of a nontrivial phase structure of the mixed SU(N)–SU(N)/Z_N lattice gauge theory were first predicted at large N in Ref. 65 on the basis of a $1/N$ expansion, which also led to the assertion[66] that at $N \geqslant 4$ the phase-transition line ends at a point C at a negative but finite value of β_A. Corresponding phase diagrams were also constructed.[66,67] The relationship between phase transitions and local minima of the action (3.16) was discussed in Ref. 68. Finally, we note that the phase diagrams generated by the Monte Carlo method agree with results calculated by the mean-field method[64] and by the more general variational method.[69]

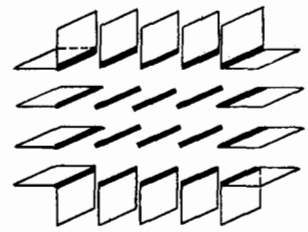

FIG. 17 A closed Z_2 vortex on a three-dimensional lattice. Links with $U_{x,\mu} \approx -1$ and plaquettes with sign $\mathrm{tr}U_p = -1$ are indicated.

f) Nature of the peak in the specific heat (continuation)

Those values of the coupling constants at which these phase transitions occur (or at which the specific heat has a peak) depend on the type of lattice action. The physical phenomenon which occurs at a phase-transition point, on the other hand, is universal and has important implications for the continuum theory. In order to take the continuum limit we need to let $\beta \to \infty$, as will be discussed in detail in the following section. It turns out that at a phase-transition point (or at a peak in the specific heat) certain types of fluctuations of the gauge field, which were important at small values of β, become "frozen."

To describe them we consider the simple case $N = 2$. We assume $U_{x,\mu} \approx -1$ on one of the links of the lattice and $U_{x,\mu} \approx 1$ on the others. We can then write

$$\text{sign tr } U_p = -1 \tag{3.19}$$

for the plaquettes which border the link with $U_{x,\mu} \approx -1$. If condition (3.19) holds for a given plaquette, then we say that it is penetrated by a Z_2 "vortex." The vortexes are conveniently examined on a three-dimensional lattice found by taking the intersection of a four-dimensional lattice with a $t = \text{const}$ plane. Figure 17 illustrates the less trivial example of a closed Z_2 vortex (a sequence of plaquettes with a negative value of sign tr U_p). The heavy lines here show links on which we have $U_{x,\mu} \approx -1$; the plaquettes which form a closed Z_2 vortex are also shown. The Z_2 vortexes may not only be closed but may also terminate on configurations for which we have

$$\prod_{p \in \partial c} \text{sign tr } U_p = -1, \tag{3.20}$$

where the product is over the six plaquettes which form the boundary of a three-dimensional cube c. A configuration of this sort, called a Z_2 "monopole," is shown in Fig. 18.

To explain the terminology, we take the naive local limit, $a \to 0$. We assume that on one of the links bounding a plaquette p we have $U_{x,\mu} = -1$, while on the three other links we have $U_{x,\mu} = +1$. We can then write

$$U_p \to \exp\left(ig_0 \oint_{\partial p} A_\mu \, dx_\mu\right) = \exp\left(ig_0 \int_p \mathbf{H} \, d\mathbf{S}\right) = -1, \tag{3.21}$$

i.e., a magnetic flux π/g passes through this plaquette. These Z_2 vortexes are thus lattice analogs of a Dirac string. Analogously, it can be stated that in a region of a space with the

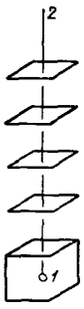

FIG. 18. A Z_2 monopole on a three-dimensional lattice. 1—Monopole source; 2—Dirac string, both found in the limit $a \to 0$.

property (3.20), from which magnetic flux emerges, there is a monopole.

Here we need to proceed cautiously, since it is well known that in the contiuum limit for the SU(2) gauge theory there are no topologically stable monopole configurations, by virtue of the condition $\pi_1[SU(2)] = 0$. However, an element of the SU(2) group can be represented as the product of elements of the SO(3) and Z_2 groups. Since the elements of Z_2 cancel out on the left side of definition (3.20) (each element appears twice: once for each of the two adjoining plaquettes from which the cube c is formed), we are left with only the product of elements of the SO(3) group, for which we have $\pi_1[SO(3)] = Z_2$. Consequently, topologically stable monopoles exist in the continuum theory. Their magnetic charge is conserved modulo 2: Z_2 monopoles.

On a lattice the difference between the SU(2) and SO(3) gauge groups is seen in the circumstance that in the SU(2) theory a Z_2 vortex carries energy, since the SU(2) action is sensitive to the sign tr U_p. In the SO(3) theory, in contrast, the Z_2 vortexes do not carry energy, and one says that the vacuum of this theory is filled with a condensate of Z_2 vortexes. A measure of the density of Z_2 vortexes is the quantity

$$\bar{E} = \frac{1}{2}\langle(1 - \operatorname{sign} \operatorname{tr} U_p)\rangle. \tag{3.22}$$

The expression which is averaged here vanishes for a vortex-free configuration and is equal to one if a vortex penetrates a given plaquette. Analogously, the density of Z_2 monopoles is given by

$$\bar{M} = \frac{1}{2}\left\langle\left(1 - \prod_{p \in \partial c} \operatorname{sign} \operatorname{tr} U_p\right)\right\rangle \tag{3.23}$$

The quantities $\bar{E}$ and $\bar{M}$ were calculated by the Monte Carlo method in Refs. 70–74. It was shown that in region I in Fig. 16 we have $\bar{E} \approx \bar{M} \approx 0.5$ [in the limit $\beta, \beta_A \to \infty$, this circumstance can be seen from definitions (3.22) and (3.23), since the sign of tr U_p takes on the values ± 1 with identical probabilities]. In other words, in vacuum there is a condensate of both vortexes and monopoles. The monopole condensate is disrupted along the line DC, and the vortex condensate is disrupted along the line AC. In region III we thus have $\bar{E} \approx \bar{M} \approx 0$, and the vacuum is free of both condensates. In region II we have $\bar{E} \approx 0.5$ and $\bar{M} \approx 0$, so that in the SO(3) theory, as we have already mentioned, the vortexes condense at arbitrary β_A, and the phase transition which is observed is related to a disruption of the monopole condensate.

In the SU(2) theory the disruption of the condensates is not of the nature of a phase transition. Figure 19 shows Monte Carlo data on $\bar{E}$ (Ref. 75) and $\bar{M}$ (Ref. 72) as functions of β for the SU(2) lattice gauge theory. The decrease at $\beta > 2.2$ is exponential, fastest in the crossover region. Furthermore, at $\beta > 2.2$ we have $\bar{M} \approx 4\bar{E}$, so that the monopoles are linked by vortexes of minimal length, for which the energy is minimal. The peak in the specific heat in the SU(2) lattice gauge theory is thus related to the freezing of Z_2 monopoles with increasing β.

If there is a monopole condensate in the vacuum, then we see an effect which is a dual of the Meissner effect in a superconductor: The electric field contracts into a tube. According to this scenario[76,77] confinement occurs in the strong-coupling region. The mechanism responsible for confinement in the weak-coupling region (and in the continuum limit) has been studied[74,78–81] by the Monte Carlo method.

4. NONPERTURBATIVE QCD CALCULATIONS BY THE MONTE CARLO METHOD

The Monte Carlo method makes it possible to derive in QCD quantities which do not depend on the details of the lattice calculations and which are pertinent to the contin-

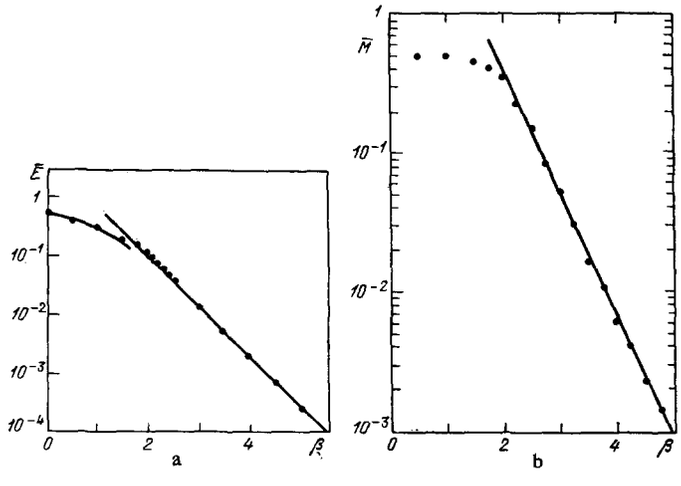

FIG. 19. Exponential decay of (a) the density of Z_2 vortexes[75] and (b) the density of Z_2 monopoles[72] in an SU(2) lattice gauge theory.

uum theory. Here we mean (dimensional) quantities such as string tensions and glueball masses, which vanish in any order of a perturbation theory in the coupling constant and which are due entirely to nonperturbative fluctuations.

The first nonperturbative calculation of this type was the calculation by Creutz[38,19] of the string tension in QCD without quarks (gluodynamics). The number of "physical" quantities which can be calculated in gluodynamics is by no means large. In addition to the string tension, the Monte Carlo method has been used to calculate the mass spectrum of colorless *gluon* bound states—glueballs[82,28,83–98]—and that temperature[99–106] at which a phase transition from a confinement phase (which prevails at a zero temperature) to a phase of a quark-gluon plasma occurs in the SU(2) and SU(3) gauge theories.

a) Dimensional transmutation

In the preceding sections we have referred frequently to the similarity of Monte Carlo calculations in lattice gauge theories to statistical physics. The most important distinction from statistical physics is that for the gauge theories the lattice is no more than an auxiliary approach used for the ultraviolet cutoff. Actually, we are interested in the results which are pertinent to the continuum limit. Let us examine how this limit is taken in QCD calculations by the Monte Carlo method.

The general recipe for taking the continuum limit of gauge theories is to let the lattice spacing go to zero: $a \to 0$. In the classical case, the coupling constant g_0^2 is fixed (Subsection 1c), but in a quantum theory, of course, the property of renormalizability has the consequence that the observables will depend on the cutoff radius a unless g_0^2 is assigned a special a dependence. For QCD this dependence is prescribed by the asymptotic-freedom formula

$$g_0^2(a) = -\frac{8\pi^2}{b \ln a\Lambda_{\text{QCD}} + (b_1/b) \ln \ln (1/a^2\Lambda_{\text{QCD}}^2)}. \tag{4.1}$$

The constants b and b_1 which appear here were calculated by perturbation theory in Refs. 3 and 107, respectively:

$$b = \frac{11}{3} N_c - \frac{2}{3} N_f, \quad b_1 = \frac{17}{3} N_c^2 - \frac{5}{3} N_c N_f - \frac{N_c^2 - 1}{2N_c} N_f; \tag{4.2}$$

here $N_c = 3$ is the number of colors for the SU(N_c) color group, and N_f is the number of types of quarks. The experimental value of the constant Λ_{QCD} is[108] $\sim$200–400 MeV.

It follows from (4.1) that in order to take the continuum limit we must simultaneously cause g_0^2 and a to approach zero in such a manner that their combination

$$\Lambda_{\text{QCD}} = \frac{1}{a} \left(\frac{16\pi^2}{bg_0^2}\right)^{b_1/b^2} e^{-8\pi^2/bg_0^2} [1 + O(g_0^2)] \tag{4.3}$$

remains constant.

Expression (4.3) could be looked at in a slightly different way. We started with the QCD Lagrangian, in which the only parameters are the interaction constant g_0 and the quark masses[1,2]:

$$\mathcal{L} = -\frac{1}{2} \operatorname{tr} F_{\mu\nu}^2 + \sum_{f=u,d,\ldots} \bar{\Psi}_f (i\hat{\nabla} - m_f) \Psi_f; \tag{4.4}$$

here $F_{\mu\nu}$ is given by (1.7), and the covariant derivative

$$\hat{\nabla} = \gamma_\mu (\partial_\mu - ig_0 A_\mu) \tag{4.5}$$

acts on Ψ_f, the field of the quark of type f with mass m_f.

As expected, Lagrangian (4.4) describes not only processes which are determined by short distances but also (for example) quark confinement. The following nontrivial problem arises immediately: For the time being we ignore the "heavy" quarks f = s,c,b,. . . , which have no effect on the confinement of the light quarks f = u,d. The masses of the light quarks are of the order of a few MeV ($m_u \approx 4.2$ MeV, $m_d \approx 7.5$ MeV). The constant g_0 is dimensionless, and the observed quark confinement radius is of the order of hundreds of reciprocal MeV.

Expression (4.3) shows how this problem can be solved. Since the quantum theory has a dimensional parameter from the outset—the cutoff radius—we can also construct the (dimensional) quantity (4.3) from it and the coupling constant. The quantity in (4.3) remains constant in the continuum limit and provides a scale for measuring the dimensional quantities which arise in the theory. In other words, the observable dimensional quantities are proportional to the corresponding power of Λ_{QCD}. For example, the quark confinement radius is

$$R_c = \text{const} \cdot \Lambda_{\text{QCD}}^{-1}, \tag{4.6}$$

and the meson masses are

$$M_1 = C_1 \Lambda_{\text{QCD}}, \tag{4.7}$$

where the (dimensionless) constants C_1 are universal (i.e., independent of g_0^2) numbers, which are determined exclusively by the quantum numbers of the meson and by N_c and N_f. This phenomenon has been labeled "dimensional transmutation."

This situation is a common property of QCD, prevailing for any regularization, including a lattice regularization. In lattice calculations the role of the cutoff radius is played by the lattice constant a. Generally speaking, there is no invariance under the rotation group. The rotational symmetry is restored, as expected, when the scale dimension for changes in the gauge fields on the lattice, the "correlation length," is considerably larger than the lattice constant.

It is convenient to introduce the dimensionless ratio

$$\xi_c = \frac{\text{correlation length}}{a}, \tag{4.8}$$

i.e., to express the correlation length in lattice units. According to dimensional transmutation, the correlation length is proportional to $\Lambda_{\text{QCD}}^{-1}$, so that at small values of g_0^2 the quantity ξ_c must depend on g_0^2 in accordance with the general expression

$$\xi_c = \text{const} \cdot \left(\frac{16\pi^2}{bg_0^2}\right)^{-b_1/b^2} e^{8\pi^2/bg_0^2}. \tag{4.9}$$

We thus see that we have $\xi_c \to \infty$ in the limit $g_0^2 \to 0$, so that the lattice structure is not manifested. At small values of g_0^2 the invariance under the rotation group should therefore be restored, and the continuum limit should set in.

It is this property which is used to take the continuum limit in Monte Carlo calculations in lattice gauge theories.

In practice, in calculations of dimensional quantities (expressed in lattice units) one attempts to follow their exponential dependence on g_0^2. If, at some g_0^2, the quantity being calculated comes to depend on g_0^2 in accordance with an expression like (4.9), we can confidently say that this quantity is pertinent to the continuum limit.

b) String tension

1) The first dimensional quantity for which nonperturbative Monte Carlo calculations were carried out is the string tension K, defined in Subsection 1f. In the original paper by Creutz,[38] K was calculated in an SU(2) gauge theory without quarks. In the actual Monte Carlo calculations, the loop average (1.34) was calculated for a square of side Ia. The results calculated for a given value of g_0^2 were described by

$$W(I, I) = \exp(A - BIa - KI^2a^2), \tag{4.10}$$

from which the value of K was extracted.

The results are shown in Fig. 20 as a plot of the dimensionless quantity a^2K as a function of $1/g_0^2$. The ordinate scale is logarithmic. The circles are the results of the Monte Carlo calculation of a^2K at the given value of g^2. We see from Fig. 20 that at small values of $1/g_0^2$ (large g_0^2) the Monte Carlo data conform to a curve (1) which corresponds to ten orders of the strong-coupling expansion [corresponding calculations for the SU(3) group were carried out in Refs. 110].

The string tension K vanishes in all orders of a perturbation theory in g_0^2. The nonvanishing value of K at small values of g_0^2 is therefore due entirely to nonperturbative effects, and by virtue of dimensional transmutation it must depend on g_0^2 in accordance with

$$a^2K = \text{const} \cdot \left(\frac{24\pi^2}{11g_0^2}\right)^{102/121} e^{-24\pi^2/11g_0^2}. \tag{4.11}$$

[Here we have used the value $b = 22/3$ for an SU(2) gauge theory without quarks ($N_c = 2, N_f = 0$).] In Fig. 20, this dependence of a^2K on $1/g_0^2$ corresponds to a family of sloping lines. They are essentially straight since in this range of g_0^2 the g_0^2 dependence of the coefficient of the exponential function is not apparent. The only adjustable parameter is the constant in (4.11); a change in this constant corresponds to a parallel translation of the line. The value of this constant is chosen for the best fit of the Monte Carlo data at small values of g_0^2.

Creutz[38] derived a best fit of the Monte Carlo data for a^2K in the region $g_0^2 < 1.9$ ($\beta = 4/g_0^2 < 2.1$), fixing the constant in the following way:

$$a^2K = \exp\left\{-\frac{24\pi^2}{11}\left[\frac{1}{g_0^2} - (0.50 \pm 0.01)\right]\right\}. \tag{4.12}$$

This expression corresponds to the sloping line 2 in Fig. 20.

In a lattice gauge theory the string tension thus turned out to be nonzero over the entire range of g_0^2 considered. This fact had been established earlier for large values of g_0^2 on the basis of the strong-coupling expansion (Subsection 1e). At $g_0^2 < 1.9$, however, where the strong-coupling expansion cannot be used, we know that the string tension is again nonzero, but now our knowledge is based only on Monte Carlo calculations. Furthermore, since the nonanalytic dependence of the tension K on g_0^2 predicted by asymptotic freedom sets in at $g_0^2 < 1.9$, there is reason to believe that the continuum limit has set in here.

This can be seen directly, by verifying that rotational symmetry is restored at $g_0^2 < 1.9$. Lang and Rebbi[111] used the Monte Carlo method to construct equipotential surfaces for the interaction between two static quarks at a given value of g_0^2. This quantity is convenient for determining whether rotational symmetry is restored, for the following reason.[112]

In the strong-coupling region ($g_0^2 \gg 1$) the force between quarks increases linearly over distance (Subsection 1e). This distance is by definition the length of the path which connects two lattice sites and which is constructed from links of the lattice. The interaction energy is thus given by

$$E(x, y, z) = K(|x| + |y| + |z|), \tag{4.13}$$

and the equipotential lines have the form shown in Fig. 21. At $g_0^2 \gg 1$ we thus have only a cubic symmetry (rotations through an angle which is a multiple of $\pi/2$ around each

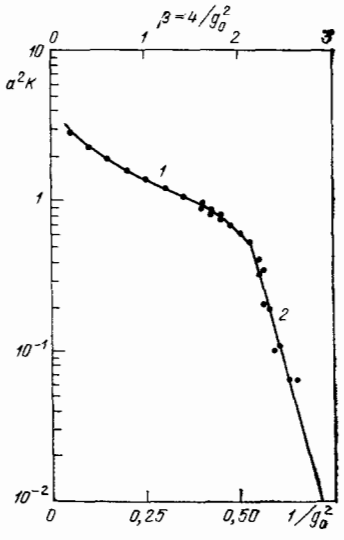

FIG. 20. String tensions calculated by the Monte Carlo method in the SU(2) theory. Curve 1—Ten orders of the strong-coupling expansion[109]; 2—expression (4.12) (this figure is taken from the paper by Creutz[38]).

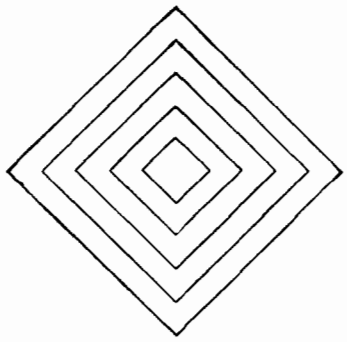

FIG. 21. Equipotential lines in the strong-coupling limit (see Subsection 4b).

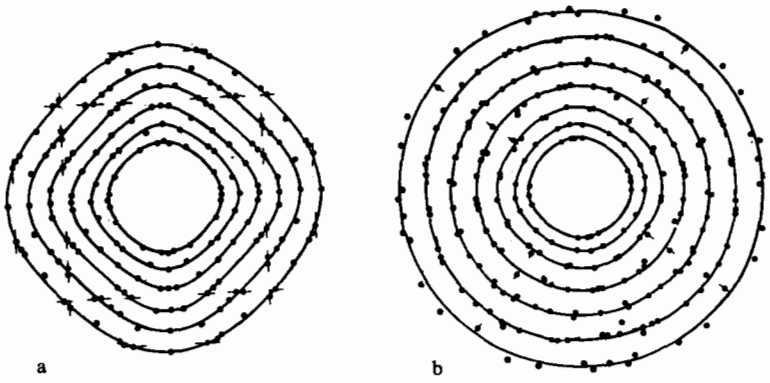

FIG. 22. Equipotential lines in the SU(2) theory according to Monte Carlo calculations. a—Coupling constant $\beta = 2$; b—$\beta = 2.25$ (this figure is taken from the paper[111] by Lang and Rebbi).

axis), not a symmetry under the complete rotation group (in which case the equipotential lines would be circles).

Figure 22 shows the Monte Carlo data of Lang and Rebbi[111] for the equipotential lines. Figure 22a shows the equipotential lines for $g_0^2 = 2$ ($\beta = 2$), and Fig. 22b shows them for $g_0^2 = 1.78$ ($\beta = 2.25$). From Fig. 22 we see that the rotational symmetry is in fact restored[1)] when we go from $g_0^2 = 2$ to $g_0^2 = 1.78$, i.e., when we pass through the point $g_0^2 = 1.9$, at which the g_0^2 dependence of the string tension starts to be described by expression (4.12). This circumstance is yet another piece of evidence that the quantities derived by the Monte Carlo method at $g_0^2 < 1.9$ are pertinent to the continuum limit.

Remarkably, the continuum limit sets in when the correlation length is only slightly greater than the lattice constant ($\xi_c = 1.5$–2.0 at $g_0^2 = 1.9$). It is for this reason that quantities pertinent to the continuum limit can be calculated by the Monte Carlo method on a lattice of finite size (and not too large). Although the number of links of the lattice in the volume ξ_c^4 is not great, we must not forget the group variables when we count the number of degrees of freedom. Furthermore, as was shown in Ref. 59, for the gauge group SU(N_c) at large N_c the spatial and group degrees of freedom are so tangled up that quantities pertinent to the continuum limit must be found on a lattice of size 1^4.

As one of the quantities characterizing the continuum SU(2) gauge theory we show in Fig. 23 the potential of the interaction between static quarks as a function of the distance according to Monte Carlo calculations.[114] This potential was calculated from Eqs. (1.46) and (1.48), which couple the potential to the loop average of $W(R, T)$ for various values of g_0^2 in the interval $1.3 \leqslant g_0^2 < 1.8$ ($3.1 > \beta > 2.2$), where the continuum limit has already set in. Both the potential and the distance are expressed in physical units, i.e., in units of $\sqrt{K}$, determined by (4.12). The various points in Fig. 23 correspond to different values of g_0^2. The fact that the results calculated for various values of g_0^2 agree shows that Eq. (4.9) is applicable. The solid curve in Fig. 23 is a description of the Monte Carlo data in the form of a Coulomb potential plus a linearly increasing potential.

The results calculated for the string tension by the Monte Carlo method show that quark confinement prevails as well as asymptotic freedom in the continuum SU(2) gauge theory. This conclusion was reached first by Creutz[37,48] and Wilson,[39] and it was later confirmed by other investigators.[19,27,28,115,116] Yet another numerical proof of this property is based on a Monte Carlo calculation[117] of the distance dependence of the effective interaction constant [see Ref. 118 regarding the SU(3) group]. Before Monte Carlo calculations were carried out the primary argument in favor of confinement had come from the results derived by Migdal[15] and Kadanoff[119] from recursion equations. Comparison with the Monte Carlo data made it possible to assess the accuracy of the approximate recursion method.[120]

2) Creutz used Eq. (4.10) to find the g_0^2 dependence of the string tension K shown in Fig. 20. The results found by this approach depend on whether the value $W(0, 0) = 1$ is incorporated, so that some of the values of g_0^2 in Fig. 20 correspond to two different values of K. Creutz subsequently suggested[19] an elegant way for finding K; the same quantity which is calculated by the Monte Carlo method is plotted directly on the curve, and no further processing is necessary. This quantity is the force $\chi(I)$ (see Subsection 1g), the force

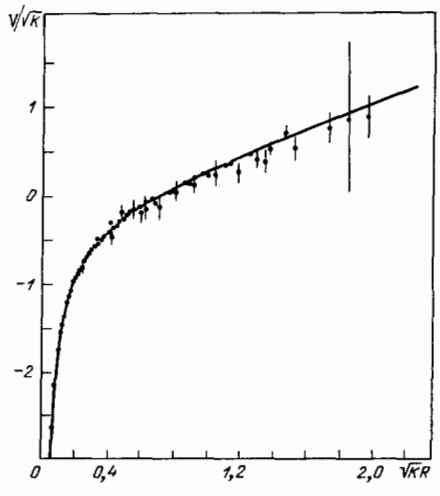

FIG. 23. Potential of the interaction between static quarks as a function of the distance in the continuum SU(2) theory. The solid curve is drawn using the expression for a Coulomb potential plus a linearly increasing potential (this figure is taken from the paper[114] by Stack).

[1)] The mechanism which is responsible for the restoration of rotational symmetry in the framework of the strong-coupling expansion is discussed in Refs. 112 and 113.

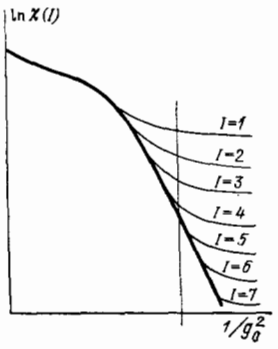

FIG. 24. Expected functional dependence of $\chi(I)$, given by (1.53), on g_0^2 for various values of I (Subsection 4b).

which test static quarks separated by the distance $I \cdot a$ exert on each other.

Before we look at the graphs with the actual results of the Monte Carlo calculations of $\chi(I)$, let us consider what we should look for on the basis of the idealized sketch on Fig. 24. Figure 24 plots $\ln\chi(I)$ as a function of $1/g_0^2$ for various values of I, conveying this functional dependence qualitatively correctly. Let us examine the behavior of χ as a function of I at some fixed $1/g_0^2$. In the strong-coupling region ($1/g_0^2 \ll 1$) the force χ is independent of the distance I (according to Subsection 1g), so that χ has the same value for all I. All the curves of $\chi(I)$ as a function of $1/g_0^2$ in Fig. 24 thus merge to form a common curve.

We now assume that $1/g_0^2$ is fixed in the weak-coupling region [i.e., $g_0^2 < 1.9$ for the SU(2) group], where the confinement radius R_c is smaller than the lattice constant a by a factor of at least a few units. The vertical line in Fig. 24 corresponds to a fixed value of $1/g_0^2$. The points at which this line intersects the curves of $\chi(I)$ versus $1/g_0^2$ for the various values of I give us the values of $\chi(I)$ for the given value of $1/g_0^2$. The largest value of χ for a given value of g_0^2 corresponds to $I = 1$. As I is increased (under the constraint $Ia \ll R_c$) the values of $\chi(I)$ fall off in accordance with a Coulomb law, and the intersection points move downward along the vertical line. As I is increased further, however, and the product Ia becomes greater than R_c, the value of $\chi(I)$ becomes independent of the distance according to Eq. (1.58), and the intersection points begin to move together. This limiting value is the value of a^2K which we are seeking.

This functional dependence of the force χ on the distance at a fixed g_0^2 thus has a simple physical interpretation: As long as the distance between the quarks is smaller than the confinement radius, the force acting between the quarks can be described by the Coulomb law. As the distance increases, the Coulomb potential gives way to a linearly increasing potential, for which the force is independent of the distance. The limiting value of the force is by definition the string tension K.

This limiting value of $\chi(I)$, calculated for various values of g_0^2, gives us the dependence of a^2K on g_0^2. A plot of the function $a^2K(g_0^2)$ is thus an envelope of the family of curves $\chi(I;g_0^2)$. This envelope is the heavy curve in Fig. 24. Everything we said above regarding how a^2K should depend on g_0^2

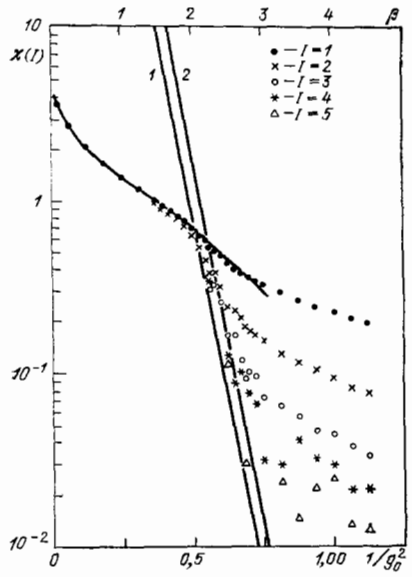

FIG. 25. Results of Monte Carlo calculations of $\chi(I)$ in the SU(2) theory. 1—$\Lambda_L = 0.013\sqrt{K}$; 2—$\Lambda_L = 0.009\sqrt{K}$. Here Λ_L is given by expression (4.15), and K is the string tension (this figure is taken from the paper[28] by Bhanot and Rebbi).

remains valid when it is determined by the method described in the present subsection. At small values of g_0^2 the envelope of the family of curves $\ln\chi(I,g_0^2)$ should therefore be a straight line with a given slope.

Curves showing the results of actual Monte Carlo calculations of $\chi(I)$ for various values of g_0^2 for the lattice gauge theories with the SU(2) and SU(3) groups agree qualitatively with the curve in Fig. 24. These curves were first obtained by Creutz,[19] and those results were subsequently reproduced in Refs. 28 and 115 for the SU(2) group and in Refs. 121, 48, 122, and 118 for the SU(3) group. To illustrate these results we show in Fig. 25 some results obtained by Bhanot and Rebbi,[28] who approximated the SU(2) group by its icosahedral subgroup $\bar{Y}$ (Subsection 2c), so that they could work on

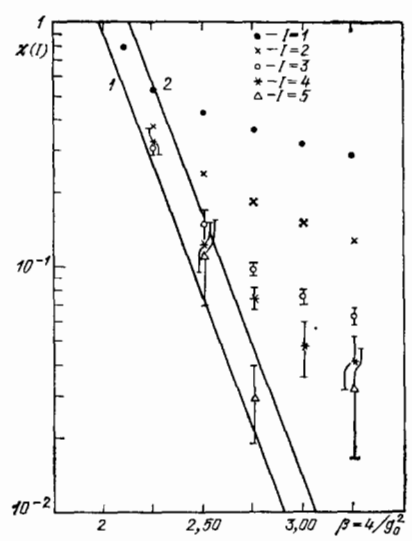

FIG. 26. The same as in Fig. 25, but on a larger scale.[28]

a lattice of size 16^4 [in this case the multiplicity of the integral evaluated by the Monte Carlo method in (1.25) is $\approx 8\cdot 10^5$]. The most interesting part of this figure is shown in larger scale in Fig. 26 along with the statistical errors in the calculated results. The sloping lines in Figs. 25 and 26 are drawn from the expression

$$\Lambda_{L_1} = (0{,}011 \pm 0{,}002)\sqrt{K},\ \text{SU (2)}, \tag{4.14}$$

where

$$\Lambda_L = \frac{1}{a}\left(\frac{24\pi^2}{11g_0^2}\right)^{51/121} e^{-12\pi^2/11g_0^2},\ \text{SU (2)}, \tag{4.15}$$

specifies that value of the parameter Λ_{QCD} which corresponds to lattice regularization. These lines are the envelopes of the family of curves in the weak-coupling region.

Corresponding calculations for the SU(3) gauge group (the largest lattice used here was the 10^4 lattice used by Pietarien[121]) yield results in agreement[2)] with the value[48,118]

$$\Lambda_L = (6 \pm 1)\cdot 10^{-3}\sqrt{K},\quad \text{SU (3)}, \tag{4.16}$$

where

$$\Lambda_L = \frac{1}{a}\left(\frac{16\pi^2}{11g_0^2}\right)^{51/121} e^{-8\pi^2/11g_0^2},\ \text{SU (3)}; \tag{4.17}$$

the indicated error here includes both the statistical error of the Monte Carlo data and the subjective error in fitting an envelope to the family of curves $\chi(I;g_0^2)$.

c) Relationship between $\sqrt{K}$ and Λ_{QCD}

As was discussed in Subsection 4a, the ratios of the dimensional physical quantities (of identical dimensionality) which arise as the result of dimensional transmutation in QCD are universal constants which can be calculated by the Monte Carlo method. For example, we can calculate the ratio of the QCD constant Λ_{QCD} and the square root of the string tension, $\sqrt{K}$. If we are interested in the absolute values of dimensional quantities we must set one of them equal to its experimental value, and then we can express the others in terms of it.

In the Monte Carlo calculations in lattice gauge theories it is customary to take the string tension from experiment. This is done in the following way. In the string model the tension K is related to the slope of the Regge trajectory, α', by

$$\sqrt{K} = \frac{1}{\sqrt{2\pi\alpha'}}. \tag{4.18}$$

This relationship is found even for a classical string (see the review of Marinov[123]). Substituting $\alpha' = 1\text{GeV}^{-2}$, and working from the slope of the $\rho - A_2 - g$ trajectory, we find

$$\sqrt{K} = 400\ \text{MeV}. \tag{4.19}$$

A similar value,[124]

$$\sqrt{K} = 430\ \text{MeV} \tag{4.20}$$

is found from a description of mesons made up of heavy quarks by a nonrelativistic potential model.

Substitution of these values of $\sqrt{K}$ into expression (4.16), obtained by the Monte Carlo method, yields

$$\Lambda_{L_1} = 2\text{—}3\ \text{MeV}. \tag{4.21}$$

It might appear at first glance that this value of Λ_L is too small and badly at odds with the experimental data available, for example, on deep inelastic scattering, since for $\Lambda_{QCD} \approx 2$–3 MeV Bjorken scaling would continue up to momenta of the order of several MeV. In fact, there is no contradiction, for the following reason.

The value of the QCD constant Λ_{QCD} generally depends on the regularization method and the gauge. One of the traditional regularization procedures of the continuum theory contains a subtraction at a symmetric point in momentum space. The value of the parameter Λ_{QCD} corresponding to this "momentum regularization" is denoted by Λ_{mom}. The quantity Λ_L in (4.16), on the other hand, is that value of Λ_{QCD} which corresponds to a lattice regularization. Hasenfratz and Hasenfratz[125] established the relationship between Λ_{mom} and Λ_L:

$$\Lambda_{mom}^{\alpha=1} = 83{,}4\Lambda_L; \tag{4.22}$$

here $\Lambda_{mom}^{\alpha=1}$ corresponds to the Feynman gauge, and the value of the constant is written for the SU(3) group. In another gauge or for another group, the 83.4 would be changed. The reason for the dependence of Λ_{QCD} on the regularization method will be discussed in Subsection 4f below.

Substitution of (4.21) into (4.22) gives us

$$\Lambda_{mom}^{\alpha=1} = 210 \pm 40\ \text{MeV}, \tag{4.23}$$

in agreement with the generally accepted phenomenological value $\Lambda_{mom}^{expt} = 200$–$350$ MeV. The first calculation of Λ_{mom} was carried out by Creutz,[19] and this was also the first calculation of a physical quantity by the Monte Carlo method.

It should be kept in mind, however, that these calculations ignored virtual quark loops. From the phenomenological standpoint this approximation is valid within an error equal to the ratio of the widths of hadron resonances to their masses, i.e., ~ 10–20%. This approximation can be justified theoretically in the approximation of a large number of colors, N_c, in which the virtual quark loops become unimportant.[126]

d) Glueball masses

The Monte Carlo method is used to calculate the masses of bound state—hadrons—in QCD. To explain the calculation method we adopt the example of glueballs: bound states of gluons which exist even in pure gluodynamics, i.e., in QCD without quarks.

The glueball masses are found by calculating the sum

[2)] After the present review had been written, some papers[154] were published with calculations of the string tension for the SU(3) gauge group on a large lattice. The ratio $\Lambda_L/\sqrt{K}$ can accordingly be found from these results by looking at the region of larger values of β. The resulting value, $\Lambda_L = (10 \pm 2)\cdot 10^{-3}\sqrt{K}$ is significantly larger than that in (4.16) and corresponds to $\Lambda_{mom} = 330 \pm 70$ MeV [cf. (4.23)]. As was shown in Ref. 155, the ratio $\Lambda_L\sqrt{K}$ is underestimated in the SU(3) theory with Wilson action (1.18) near the crossover region for the same reason that expression (4.43) becomes incorrect near the end point of the phase diagram in the SU(2)-SO(3) theory with the mixed action (3.16) (Subsection 4f). The β dependence of the ratio $\Lambda_L/\sqrt{K}$ does not, however, have any significant effect on the values of other dimensional quantities found by the Monte Carlo method (e.g., glueball masses and deconfinement temperatures).[155]

over the lattice sites in one "time" layer $t \equiv x_4$ of the coupled correlation function of two operators $O(\mathbf{x}, t)$ with the quantum number of the given glueball:

$$\Delta(t) = \sum_{\mathbf{x}} \{\langle O(\mathbf{x}, t) O(0, 0)\rangle - \langle O(0, 0)\rangle^2\}. \quad (4.24)$$

In the simplest version, $O(\mathbf{x}, t)$ is chosen in the form

$$O(\mathbf{x}, t) = \operatorname{tr} U_p, \quad (4.25)$$

where the plaquette p is constructed at the point $\mathbf{x}, t$. Substituting a sum over intermediate states into definition (4.24) (by analogy with Subsection 1f), we find

$$\Delta(t) = \sum_{n \neq 0} |\langle O(\mathbf{0}, 0)|n\rangle|^2 e^{-Mnt}. \quad (4.26)$$

The summation here is over all the glueball excitations with masses M_n. The vacuum state ($n = 0$) has cancelled out, since a coupled correlation function appears in definition (4.24).

Since the lower state is predominant in the sum (4.26) at large t, the mass of this state can be determined from the argument of the exponential function describing the decrease in $\Delta(t)$ with increasing t. The mass of the lightest glueball was calculated by a method of this type only in the early papers,[82,28] where this value was determined somewhat crudely for the SU(2) gauge group. The reason for this circumstance is that the correlation function $\Delta(t)$ is small in absolute value in the region dominated by the lower state, and a great deal of computer time is required to extract the signal from the statistical noise. Some subtler methods were subsequently developed for calculating glueball masses.

The method most popular today is a variational method proposed by Wilson (see also Ref. 127), which has not only yielded reliable values of the mass of the lightest glueball in the case of the SU(3) gauge group (with the quantum numbers 0^{++}) but has also made it possible to calculate the masses of glueballs with other quantum numbers. A calculation procedure using the variational method was initially worked out[86–88] for the SU(2) gauge group and was subsequently applied[89–91,93–95] to the SU(3) group.

The basic idea of the variational method for calculating glueball masses is to adopt as $O(\mathbf{x}, t)$ the linear combination

$$O(\mathbf{x}, t) = \sum_i A_i \operatorname{tr} U_{C_i}, \quad (4.27)$$

where the loops C_i pass through the point $\mathbf{x}, t$, and the A_i are constants. For given value of the constants one calculates the quantity

$$m(t) = \ln \frac{\Delta(t-a)}{\Delta(t)}, \quad (4.28)$$

and then performs a minimization with respect to the A_i; i.e., the A_i are chosen to achieve the smallest possible value of $m(t)$ for the given choice of operators on the right side of (4.27).

From expansion (4.26) we see that all the glueball states make a positive contribution to $\Delta(t)$. The rate at which $\Delta(t)$ falls off with increasing t [the quantity $m(t)$] is thus lowest for that operator $O(\mathbf{x}, t)$ which creates the lightest glueball at the point $\mathbf{x}, t$ from vacuum. The variational method is an algorithm for constructing this operator.

For an operator which creates the lightest glueball from vacuum we are left with only a single term on the right side of expansion (4.26), so that $m(t)$ is identical for all t and equal to the mass. We can thus use $t = 1$ to calculate the mass. The quantity $\Delta(0)$ is related to the square of the wave function and is also of interest.

In actual fact it is not possible on a lattice of finite size to construct an operator which creates the lightest glueball exactly since the number of operators considered in expansion (4.27) is finite. Accordingly, there always remains some admixture of higher-lying states. To estimate the admixture we minimize $m(1)$, $m(2)$, $m(3)$, etc., separately and compare the results. The calculations show that for lattices of this size $m(3)$ is only slightly smaller than $m(1)$. At any rate, $m(1)$ is an upper limit on the mass of the lightest glueball.

We turn now to the results calculated for the glueball masses. For the SU(2) gauge group an exponential dependence of the mass of the lightest glueball on $1/g_0^2$ was reliably established in Refs. 86, 92, and 95, where calculations were carried out by a variational method, and also in Ref. 96, where the result was determined from the change in the loop averages upon a change in boundary conditions. The results agree with the value

$$m(0^+) = (200 \pm 25)\Lambda_L = (2{,}2 \pm 0{,}3)\sqrt{K}, \text{ SU (2)}, \quad (4.29)$$

where we have used (4.14).

An exponential dependence of $m(0^{++})$ on $\beta = 6/g_0^2$ was studied for the SU(3) gauge group in Refs. 89, 94, 98, and 95. The results agree with the value[94]

$$m(0^{++}) = (280 \pm 30)\Lambda_L, \text{ SU (3)}. \quad (4.30)$$

Using (4.21) for Λ_L, we have, in physical units,

$$m(0^{++}) = 700\text{—}750 \text{ MeV}. \quad (4.31)$$

The variational method can be used to calculate the mass spectrum of glueballs with various quantum numbers. For this purpose the variational principle is applied to the operators which are orthogonal to the operator constructed previously for the state of quantum numbers 0^{++}. The operators are classified in accordance with representations of the cubic group, which transforms into the rotation group in the continuum limit.

The exponential dependence of $m(2^{++})$ on β was studied in Refs. 92 and 95, where the following value was found:

$$m(2^{++}) = (1620 \pm 100) \text{ MeV}. \quad (4.32)$$

The mass spectrum of glueballs with other quantum numbers was calculated in Refs. 90, 91, and 93–95. The results found in Ref. 95 are

$$\begin{aligned} m(0^{-+}) &= (1420 \pm {}^{240}_{170}) \text{ MeV}, \\ m(0^{--}) &= (2880 \pm 300) \text{ MeV}, \\ m(1^{-+}) &= (1730 \pm 220) \text{MeV}, \\ m(1^{+-}) &= (2980 \pm 300) \text{ MeV}. \end{aligned} \quad (4.33)$$

These results are not as reliable as the values in (4.31) and (4.32) for $m(0^{++})$ and $m(2^{++})$, since the exponential dependence on β was not studied. We can at any rate take it to be an established fact that $m(0^{++})$ is anomalously small in pure gluodynamics: smaller by a factor of at least two than the

other masses (see Ref. 128 regarding calculations by means of a strong-coupling expansion).

Although the results obtained clearly refer to the continuum limit, it is not known how these results would be changed by the incorporation of quarks, since glueballs (the 0^{++} glueballs, for example) may mix extensively with quark states. From this standpoint we would be particularly interested in seeing calculations in pure gluodynamics of the masses of "odd" glueballs, e.g., those with quantum numbers 1^{-+} and 0^{--}, which do not mix with two-quark states, so that their masses will presumably not change greatly when quarks are incorporated. The masses calculated for the low-lying odd glueballs[93,95] show that the 1^{-+} glueball is relatively light [see Eq. (4.33)].

e) Deconfinement temperature

Although a linearly increasing potential arises between static quarks with increasing distance in the SU(2) and SU(3) gauge theories, this property cannot persist at arbitrarily high temperatures. As Polyakov and Susskind[129] have discussed, a phase transition from a phase of hadronic matter to a phase of a quark-gluon plasma must occur at some temperature T_c: the deconfinement temperature. The temperature T_c was calculated by the Monte Carlo method in Refs. 99–101, 83, and 104–106 for the SU(2) gauge group and in Refs. 102–104 for the SU(3) group.

We know quite well that a description of a system at a finite temperature T_c requires examining a lattice which is infinite in the three spatial directions with a finite number of spacings n_t along the time axis t, along which periodic boundary conditions are imposed. The temperature is related to n_t by

$$T = (an_t)^{-1}, \tag{4.34}$$

where a is the lattice constant.

At a finite temperature there is yet another gauge-invariant quantity: the trace of the product of matrices $U_{x,\mu}$ along a line passing through the lattice parallel to the t axis. Gauge invariance is assured by periodic boundary conditions. Quantities of this type are denoted by $L_{\mathbf{x}}$ since the spatial coordinates of all the links of the lattice forming the given line are identical and equal to $\mathbf{x}$. Repeating the arguments in Subsection 1f, we see that the quantity

$$F_0 = -\frac{1}{an_t}\ln\langle L_{\mathbf{x}}\rangle, \tag{4.35}$$

where the expectation value $\langle L_{\mathbf{x}}\rangle$ is determined with the help of general expression (1.32), represents the change in the free energy of the lattice system upon the introduction of a static quark at the point $\mathbf{x}$. To calculate the deconfinement temperature by the Monte Carlo method one makes use of the fact that in the confinement phase F_0 is infinite, so that we have $\langle L_{\mathbf{x}}\rangle = 0$, while the phase with unconfined quarks F_0 and $\langle L_{\mathbf{x}}\rangle$ are finite. In practice, for a given n_t one calculates $\langle L_{\mathbf{x}}\rangle$ for various values of the charge g_0^2 and determines that value g_c^2 at which $\langle L_{\mathbf{x}}\rangle$ becomes nonzero (under the condition $g_0^2 < g_c^2$). The calculations are then repeated with other values of n_t. In this manner, g_c^2 is found as a function of n_t, or, equivalently, $T_c \cdot a$ is found as a function of g_c^2.

Since T_c is a dimensional quantity, it must be proportional to Λ_L, according to dimensional transmutation, and at small values of g_c^2 it must depend on $1/g_c^2$ exponentially if the resulting value T_c is to refer to the continuum limit. This property was established for the SU(2) gauge group in Refs. 98–101, where the following relationship was found between T_c and Λ_L:

$$T_c = (38\text{—}43)\,\Lambda_L = (0{,}43\text{—}0{,}47)\sqrt{K}, \quad \text{SU (2)} \tag{4.36}$$

[(4.14) has been used here]. Correspondingly, an exponential dependence of T_c on $1/g_c^2$ has been investigated also for the SU(3) gauge group, and the following result has been derived[102–104]:

$$T_c = (75\text{—}83)\,\Lambda_L \approx 200 \text{ MeV}, \quad \text{SU (3)}, \tag{4.37}$$

where (4.16) has been used for Λ_L.

Monte Carlo calculations have also shown[83,103] that near T_c the temperature dependence of the energy density of the system, $\varepsilon(T)$, changes abruptly from the value corresponding to hadronic matter to that corresponding for a gluon plasma. At $T > 2T_c$, we can describe $\varepsilon(T)$ well by the Stefan-Boltzmann law

$$\varepsilon(T) = \frac{\pi^2}{15}T^4(N_c^2 - 1) \tag{4.38}$$

with the coefficient calculated for an ideal gas of free massless gluons. This change in the behavior of $\varepsilon(T)$ has been exploited[83,103] to calculate T_c.

How well (4.37) agrees with experiment can be tested on the basis of cosmological consequences and also in experiments on heavy-ion accelerators (see the review by Feĭnberg[130]).

f) Universality

As we mentioned in Subsection 3e, quantities referring to the continuum limit must not depend on the type of lattice action used in Monte Carlo calculations, and they must be identical for, say, actions (1.18) and (3.16). This property is called "universality," and such actions are said to belong to the same universality class.

In calculations with various types of action, however, the constants which relate, say, Λ_L and $\sqrt{K}$ [see (4.16)] are different. In order to test universality we must interrelate the parameters Λ_L corresponding to different actions and show that $\sqrt{K}$ does not change in the process. This difference in the value of Λ_L is caused by the same factor as the difference in the value of Λ_L for the Wilson action and Λ_{mom} given by (4.22). Let us first see how this relation arises.

To find the relationship between Λ_{mom} and Λ_L, Hasenfratz and Hasenfratz[125] used a lattice perturbation theory to calculate the gluon propagator and the three-gluon vertex at a symmetric point in momentum space, $p_1^2 = p_2^2 = (p_1 - p_2)^2 = M^2$, using the single-loop approximation. The renormalized charge $g(M)$ is expressed in terms of g_0 and the renormalization constants Z_3 (of the propagators) and Z_1 (of the vertex) in the standard way:

$$g^2(M) = g_0^2 Z_3^3 Z_1^{-2}. \tag{4.39}$$

Substituting the values of Z_1 and Z_3 calculated in the single-

loop approximation, Hasenfratz and Hasenfratz derived the following expression for the SU(3) group in the Feynman gauge:

$$g^2(M) = g_0^2\left[1 + g_0^2\left(\frac{11}{8\pi^2}\ln\frac{\pi}{aM} + 0{,}457\right)\right]. \quad (4.40)$$

On the right side of this expression we have shown only those terms which remain finite in the limit $a \to 0$. All the noncovariant terms cancel out in this limit.

It should be noted that the coefficient of the logarithm in (4.40) is the same as the asymptotic-freedom coefficient b. This agreement shows that in the limit $a \to 0$ not only does the classical action (1.18) convert into the action of the continuum theory, but there is also a correspondence between the results calculated by perturbation theory. The constant terms, which depend on the regularization method, differ, giving rise to differences in the values of the parameters Λ. Expression (4.22) is derived by substituting expression (4.40) into the definition

$$\Lambda_{\text{mom}} \equiv M\left(\frac{16\pi^2}{11g^2(M)}\right)^{51/121} e^{-8\pi^2/11g^2(M)}\left[1 + O(g^2(M))\right]$$
$$= \pi e^{8\pi^2/11\cdot 0{,}475}\Lambda_{\text{L}}, \quad (4.41)$$

where Λ_{L} is given by Eq. (4.17).

The calculations which lead to (4.40) are quite involved. Along with the oridinary diagrams there are some diagrams with additional vertices, which are coupled with other terms of the series expansion of U_p. For example, the Lagrangian obtained in the limit $a \to 0$ takes the following form in the g_0^2 order:

$$\mathcal{L} = \frac{1}{2}\operatorname{tr} F_{\mu\nu}^2 - \frac{C_4}{4!} g_0^2 a^4 \frac{1}{2}\operatorname{tr} F_{\mu\nu}^4, \quad (4.42)$$

where we have $C_4 = 1$ for the action (1.18). Although the second term is propertional to a^4, it gives rise to "tadpole" diagrams, which diverge as a^{-4}, so that their contribution is finite. These are the diagrams which make the numerically largest contribution to the ratio $\Lambda_{\text{mom}}/\Lambda_{\text{L}}$.

The differences between the values of Λ_{L} for various types of lattice action are due entirely to differences in the coefficients C_4 [for example, we have $C_4 = 1 + 6\beta_A/(\beta + 2\beta_A)$ for the mixed action (3.16) with the SU(2) group]. The ratio of parameters Λ_{L} can be calculated most simply by the lattice version of the background-field method.[131] Essentially all we need to do here is to determine the coefficient of one of the tadpole diagrams. The answer is[132,133] [for the SU(2) group]

$$\frac{\Lambda_{\text{L}}'}{\Lambda_{\text{L}}^{\text{Wilson}}} = \exp\left[\frac{5\pi^2}{44}(1 - C_4)\right]. \quad (4.43)$$

There are corrections of $O(g_0^2)$ to this expression, and these corrections may be large if g_0^2 is not small enough. Some of them (the dominant ones) were calculated in Ref. 134.

Monte Carlo calculations with actions of other types have been carried out for the string tension,[46,116,133] glueball masses,[87,97] and the deconfinement temperature.[105,106] It turns out that for the versions of the lattice action proposed by Manton[135] and Villain (see Ref. 136) universality holds even when we use the simple relation (4.43). For the mixed action (3.16), however, the use of (4.43) near the end point of the phase diagram (Fig. 16) has led[133] to physical quantities differing by a factor of four from the results calculated with the Wilson action. It was shown in Refs. 106 and 137–140 that relation (4.43) actually does not hold near the end point of the phase diagram. A nonperturbative calculation of the ratio of parameters Λ_{L} has shown[140] that universality also holds for the mixed action. Consequently, the quantities which are pertinent to the continuum limit actually do not depend on the type of lattice action used in their calculations by the Monte Carlo method. It is nevertheless better to use the Wilson action, than, say, the mixed action at $\beta_A > 0$, since the g_0^2 dependence of Λ_{L} is described well by simple expression (4.15) for the Wilson action in the region in which the Monte Carlo calculations are carried out.

INSTEAD OF A CONCLUSION

We have seen how the Monte Carlo method is used to study gauge theories on a lattice, including quantum chromodynamics without quarks. The results are quite reliable, although it remains to be seen whether changes will result from a decrease in the lattice spacing or an increase in the spatial dimension of the lattice. The dimensional quantities (string tensions, glueball masses, and deconfinement temperatures) calculated by this method in QCD without quarks have the correct renormalization-group behavior and refer to the continuum theory.

In addition to the quantities which were discussed more or less in detail in Section 4, the size of the gluon condensate[141,142] and the correlation function for the topological charge density[143,144] have been calculated by the Monte Carlo method in QCD without quarks. There is some uncertainty in the calculations of these quantities because of the particular way in which they are defined on a lattice.

We have not taken up Monte Carlo calculations in QCD with quarks. Methods have been developed[145] for incorporating quarks in Monte Carlo calculations. The most interesting calculations in this direction are calculations[85,146–149] by these methods of the mass spectrum of hadrons made up of quarks. The first calculations were carried out in the pioneering studies by Hamber and Parisi,[85] Marinari *et al.*, and Hamber *et al.*[146] (see also the more recent studies in Refs. 148 and 149) in an approximation which incorporated only the valence quarks and ignored virtual ("sea") quarks; alternatively, the virtual quarks have been taken into account by the approximate method of Ref. 147. Calculations have been carried out on lattices ranging in size from $5^3 \times 10$ to $10^3 \times 20$, and the masses found have depended slightly on the lattice size. The masses of low-lyingy ordinary and strange mesons and baryons and certain other quantities have been calculated. The resulting masses agree within the errors with experimental results (the agreement is slightly better for the larger lattices), although the errors are quite large, about $\pm$ 150 MeV. These errors will decrease significantly, possibly in the immediate future, as a result of the refinement of calculation methods, the increase in the statistical base, and the incorporation of virtual quarks. (In some first studies in this direction, virtual quarks have been taken into account exactly[150,151] and approximately[152] in Monte Carlo calculations.)

Doubt has been expressed[153] whether reliable results for QCD with quarks can be achieved at all on lattices of such small dimensions as were used in Refs. 85 and 148. Any substantial increase in the lattice size would require significant improvements in computer speed and memory. As it is, the hadron-mass calculations which are presently being carried out are straining the existing computational capabilities. By way of example, the calculations carried out by Lipps *et al.*[148] required about 30 h on a Cray 1S computer (the cost of this much computer time is estimated to be about $100 000). Nevertheless, the effort to increase lattice size is continuing, and calculations on even larger lattices are planned for the immediate future.

I wish to thank M. I. Polikarpov for useful comments and for assistance in writing Section 3.

[1]H. Fritzsch and M. Gell-Mann, in: Proceedings of the Sixteenth International Conference on High Energy Physics, Vol. 2, Batavia, 1972, p. 135; H. Fritzsch, M. Gell-Mann, and H. Leutwyler, Phys. Lett. **B47**, 365 (1973); S. Weinberg, Phys. Rev. Lett. **31**, 494 (1973).
[2]H. D. Politzer, Phys. Rep. **C14**, 129 (1974); W. Marciano and H. Pagels, Phys. Rep. **C36**, 139 (1978); M. B. Voloshin and K. A. Ter-Martirosyan, Teoriya kalibrovochnykh vzaimodeĭstviĭ élementarnykh chastits (Theory of Gauge Interactions of Elementary Particles), Énergoatomizdat, Moscow, 1984.
[3]D. Gross and F. Wilczek, Phys. Rev. Lett. **30**, 1343 (1973); H. D. Politzer, Phys. Rev. Lett. **30**, 1346 (1973).
[4]A. I. Vaĭnshteĭn, M. B. Voloshin, V. I. Zakharov, V. A. Novikov, L. B. Okun', and M. A. Shifman, Usp. Fiz. Nauk **123**, 217 (1977) [Sov. Phys. Usp. **20**, 796 (1977)]; V. A. Novikov, L. B. Okun, M. A. Shifman, A. I. Vainshtein, M. B. Voloshin, and V. I. Zakharov, Phys. Rep. **C41**, 3 (1978).
[5]M. A. Shifman, A. I. Vainshtein, and V. I. Zakharov, Nucl. Phys. **B147**, 385, 448 (1979); A. I. Vaĭnshteĭn, V. I. Zakharov, V. A. Novikov, and M. A. Shifman, in: Élementarnye chastitsy. Vos'maya shkola fiziki ITÉF (Elementary Particles. Eighth School of Physics of the Institute of Theoretical and Experimental Physics), No. 1, Énergoizdat, Moscow, 1981, p. 5.
[6]B. L. Ioffe, Nucl. Phys. **B188**, 317 (1981); B. L. Ioffe, in: Élementarnye chastitsy. Desyataya shkola fiziki ITÉF (Elementary Particles. Tenth School of Physics of the Institute of Theoretical and Experimental Physics), No. 3, Énergoatomizdat, Moscow, 1983, p. 64.
[7]Yu. M. Makeenko and A. A. Migdal, Nucl. Phys. **B188**, 269 (1981); A. A. Migdal, Nucl. Phys. **B189**, 253 (1981); Yu. M. Makeenko, in: Gauge Theories of the Eighties (ed. R. Raitio and J. Lindfors), Springer-Verlag, New York, 1983, p. 67.
[8]A. A. Slavnov and L. D. Faddeev, Vvedenie v kvantovuyu teoriyu kalibrovochnykh poleĭ (Introduction to the Quantum Theory of Gauge Fields), Nauka, Moscow, 1978; V. N. Popov, Kontinual'nye integraly v kvantovoĭ teorii polya i statisticheskoĭ fizike (Path Integrals in Quantum Field Theory and Statistical Physics), Atomizdat, Moscow, 1976.
[9]J. D. Bjorken and S. D. Drell, Relativistic Quantum Mechanics, McGraw-Hill, New York, 1964 (Russ. Transl. Vol. 2, Nauka, Moscow, 1978).
[10]K. G. Wilson, Phys. Rev. **D10**, 2445 (1974).
[11]A. M. Polyakov, Phys. Lett. **B59**, 79 (1975).
[12]F. J. Wegner, J. Math. Phys. **12**, 2259 (1971).
[13]J. Kogut and L. Susskind, Phys. Rev. **D11**, 395 (1975).
[14]R. Balian, J. M. Drouffe, and C. Itzykson, Phys. Rev. **D10**, 3376 (1975); **D11**, 2098, 2104 (1975).
[15]A. A. Migdal, Zh. Eksp. Teor. Fiz. **69**, 810 (1975) [Sov. Phys. JETP **42**, 413 (1975)].
[16]K. Osterwalder and E. Seiler, Ann. Phys. (NY) **110**, 440 (1978).
[17]L. D. Faddeev and V. N. Popov, Phys. Lett. **B25**, 29 (1967).
[18]V. N. Gribov, in: Fizika élementarnykh chastits. Materialy XII zimneĭ shkoly LIYaF (Physics of Elementary Particles. Proceedings of the Twelfth Winter School of the Leningrad Institute of Nuclear Physics), No. 1, LIYaF Akad. Nauk SSSR, 1977, p. 147; Nucl. Phys. **B139**, 1 (1978).
[19]M. Creutz, Phys. Rev. Lett. **45**, 313 (1980).
[20]A. M. Polyakov, Nucl. Phys. **B164**, 171 (1980); J.-L. Gervais and A. Neveu, Nucl. Phys. **B163**, 189 (1980); V. S. Dotsenko and S. N. Vergeles, Nucl. Phys. **B169**, 527 (1980); I. Ya. Aref'eva, Pis'ma Zh. Eksp. Teor. Fiz. **31**, 421 (1980) [JETP Lett. **31**, 393 (1980)]; R. A. Brandt, F. Neri, and M. Sato, Phys. Rev. **D24**, 879 (1981).
[21]K. G. Wilson, in: New Developments in Quantum Field Theory and Statistical Mechanics (ed. M. Levy and P. Mitter), Plenum Press, New York, 1977.
[22]M. Creutz, L. Jacobs, and C. Rebbi, Phys. Rev. Lett. **42**, 1390 (1979).
[23]M. Creutz, L. Jacobs, and C. Rebbi, Phys. Rev. **D20**, 1915 (1979).
[24]C.-P. Yang, in: Proceedings of Symposia in Applied Mathematics, Am. Math. Soc., Vol. 15, Providence, RI, 1963, p. 351.
[25]K. Binder (editor), Monte Carlo Methods in Statistical Physics (Russ. Transl. Mir, Moscow, 1982).
[26]C. Rebbi, Phys. Rev. **D21**, 3350 (1980).
[27]D. Petcher and D. Weingarten, Phys. Rev. **D22**, 2465 (1980).
[28]G. Bhanot and C. Rebbi, Nucl. Phys. **B180** [FS2], 469 (1981).
[29]G. Bhanot and C. Rebbi, Phys. Rev. **D24**, 3319 (1981).
[30]G. Bhanot, Phys. Lett. **B108**, 337 (1982).
[31]P. Lisboa and C. Michael, Phys. Lett. **B113**, 303 (1982).
[32]L. Jacobs and C. Rebbi, J. Comput. Phys. **41**, 203 (1981).
[33]G. Bhanot, C. Lang, and C. Rebbi, Comput. Phys. Commun. **25**, 275 (1982).
[34]R. W. B. Ardill and K. J. M. Moriarty, Comput. Phys. Commun. **24**, 127 (1981).
[35]D. Barkai and K. J. M. Moriarty, Comput. Phys. Commun. **25**, 57 (1982).
[36]R. W. B. Ardill, M. Creutz, and K. J. M. Moriarty, Comput. Phys. Commun. **29**, (1983).
[37]M. Creutz, Phys. Rev. Lett. **43**, 553 (1979).
[38]M. Creutz, Phys. Rev. **D21**, 2308 (1980).
[39]K. G. Wilson, in: Recent Progress in Gauge Theories (ed. G. 't Hooft *et al.*), Plenum Press, New York, 1980, p. 243.
[40]M. Creutz, Phys. Rev. Lett. **46**, 1441 (1981).
[41]M. Bohr and K. J. M. Moriarty, Phys. Lett. **B104**, 217 (1981); K. J. M. Moriarty, Phys. Lett. **B106**, 130 (1981); M. Creutz and K. J. M. Moriarty, Phys. Rev. **D25**, 1724 (1982).
[42]M. Creutz and K. J. M. Moriarty, Phys. Rev. **D25**, 610 (1982); Nucl. Phys. **B210** [FS6], 59, 377 (1982).
[43]I. G. Halliday and A. Schwimmer, Phys. Lett. **B101**, 327 (1981).
[44]J. Greensite and B. Lautrup, Phys. Rev. Lett. **47**, 9 (1981).
[45]M. Creutz and K. J. M. Moriarty, Nucl. Phys. **B210**[FS6], 50 (1982).
[46]G. Bhanot and M. Creutz, Phys. Rev. **D24**, 3212 (1981).
[47]R. W. B. Ardill, M. Creutz, and K. J. M. Moriarty, Brookhaven Preprint BNL 32568, 1982.
[48]M. Creutz and K. J. M. Moriarty, Phys. Rev. **D27**, 2166 (1982).
[49]M. Creutz, Phys. Rev. **D21**, 1006 (1980).
[50]B. Lautrup and M. Nauenberg, Phys. Lett. **B95**, 63 (1980).
[51]G. Bhanot, Phys. Rev. **D24**, 461 (1981).
[52]H. Hamber, Phys. Rev. **D24**, 941 (1981).
[53]C. P. Korthals-Altes, Nucl. Phys. **B142**, 315 (1978); T. Yoneya, Nucl. Phys. **B144**, 195 (1978); Al. B. Zamolodchikov, Zh. Eksp. Teor. Fiz. **75**, 341 (1978) [Sov. Phys. JETP **48**, 168 (1978)].
[54]S. Elitzur, R. Pearson, and J. Shigemitsu, Phys. Rev. **D19**, 3698 (1979); D. Horn, M. Weinstein, and S. Yankielowicz, Phys. Rev. **D19**, 3715 (1979); A. Ukawa, P. Windey, and A. H. Guth, Phys. Rev. **D21**, 1013 (1980).
[55]R. Savit, Phys. Rev. Lett. **39**, 55 (1977); T. Banks, R. Myerson, and J. Kogut, Nucl. Phys. **B129**, 493 (1977); A. Guth, Phys. Rev. **D21**, 2291 (1980); J. Fröhlich and T. Spencer, Commun. Math Phys. **83**, 411 (1982).
[56]M. Falcioni, E. Marinari, M. L. Pacielo, G. Parisi, and B. Taglienti, Phys. Lett. **B102**, 270 (1981); Nucl. Phys. **B190**[FS3], 782 (1981).
[57]B. Lautrup and M. Nauenberg, Phys. Rev. Lett. **45**, 1755 (1981).
[58]M. Nauenberg, T. Schalk, and R. Brower, Phys. Rev. **D24**, 548 (1981).
[59]T. Eguchi and H. Kawai, Phys. Rev. Lett. **48**, 1063 (1982); G. Bhanot, U. Heller, and H. Neuberger, Phys. Lett. **B113**, 47 (1982); G. Parisi, Phys. Lett. **B112**, 463 (1982); D. Gross and Y. Kitazawa, Nucl. Phys. **B206**, 440 (1982).
[60]G. Bhanot, U. Heller, and H. Neuberg, Phys. Lett. **B115**, 237 (1982); M. Okawa, Phys. Rev. Lett. **49**, 75 (1982); G. Bhanot and K. J. M. Moriarty, Phys. Lett. **B122**, 271 (1983).
[61]A. Gonzalez-Arroyo and M. Okawa, Phys. Lett. **B120**, 174 (1983); Phys. Rev. **D27**, 2397 (1983).
[62]F. Green and S. Samuel, Phys. Lett. **B103**, 48 (1981); Nucl. Phys. **B194**, 107 (1981).
[63]J. Greensite and B. Lautrup, Phys. Lett. **B104**, 41 (1981); P. Cvitanovič, J. Greensite, and B. Lautrup, Phys. Lett. **B105**, 197 (1981); H. Flyvb-

jerg, B. Lautrup, and J. B. Zuber, Phys. Lett. **B110**, 279 (1982); B. Lautrup, Preprint NBI-HE-82-8, Copenhagen, 1982; V. F. Müller and W. Rühl, Nucl. Phys. **B210**[FS6], 289 (1982); V. F. Müller, T. Raddatz, and W. Rühl, Phys. Lett. **B122**, 148 (1983).
[64]J. M. Drouffe, Phys. Lett. **B105**, 46 (1981); D. J. Pritchard, Phys. Lett. **B106**, 193 (1981); T.-L. Chen, C.-I. Tan, and X.-T. Zheng, Phys. Lett. **B109**, 383 (1982); M. C. Ogilvie and A. Horowitz, Nucl. Phys. **B215**[FS7], 249 (1983).
[65]Yu. M. Makeenko and S. B. Khokhlachev, Zh. Eksp. Teor. Fiz. **80**, 448 (1981) [Sov. Phys. JETP **53**, 228 (1981)]; S. B. Khokhlachev and Yu. M. Makeenko, Phys. Lett. **B101**, 403 (1981).
[66]Yu. M. Makeenko and M. I. Polikarpov, Nucl. Phys. **B205**[FS5], 386 (1982).
[67]S. Samuel, Phys. Lett. **B112**, 237 (1982); **122**, 287 (1983).
[68]C. P. Bachas and R. F. Dashen, Nucl. Phys. **B210**[FS6], 583 (1982).
[69]X.-T. Zheng, C.-I. Tan, and T.-L. Chen, Phys. Rev. **D26**, 2843 (1982).
[70]I. G. Halliday and A. Schwimmer, Phys. Lett. **B102**, 337 (1981).
[71]R. C. Brower, D. A. Kessler, and H. Levine, Phys. Rev. Lett. **47**, 621 (1981).
[72]R. C. Brower, D. A. Kessler, and H. Levine, Nucl. Phys. **B205**[FS5], 77 (1982).
[73]L. Caneschi, I. G. Halliday, and A. Schwimmer, Nucl. Phys. **B200**[FS4], 409 (1982).
[74]G. Mack and E. Pietarinen, Nucl. Phys. **B205**[FS5], 141 (1982).
[75]Yu. M. Makeenko, M. I. Polikarpov, and A. I. Veselov, Phys. Lett. **B118**, 133 (1982).
[76]G. 't Hooft, Nucl. Phys. **B138**, 1 (1978); **153**, 141 (1979); cited in Ref. 39; S. Mandelstam, Phys. Rev. **D19**, 2391 (1979).
[77]G. Mack and V. B. Petkova, Ann. Phys. (NY) **123**, 447 (1979); **125**, 117 (1980); Z. Phys. C **12**, 177 (1982); G. Mack, cited in Ref. 39.
[78]T. DeGrand and D. Toussaint, Phys. Rev. **D22**, 2478 (1980); **D24**, 466 (1981).
[79]J. Groenveld, J. Jurkiewicz, and C. P. Korthals-Altes, Phys. Lett. **B92**, 312 (1980); Physica Scripta **23**, 1022 (1981).
[80]G. Mack, Phys. Rev. Lett. **45**, 1378 (1980); G. Mack and E. Pietarinen, Phys. Lett. **B94**, 397 (1980).
[81]T. I. Belova, Yu. M. Makeenko, M. I. Polikarpov, and A. I. Veselov, Nucl. Phys. **B230**[FS10], 473 (1984).
[82]B. Berg, Phys. Lett. **B97**, 401 (1980); J. Engels, F. Karsch, H. Satz, and I. Montvay, Phys. Lett. **B102**, 332 (1981).
[83]J. Engels, F. Karsch, H. Satz, and I. Montvay, Nucl. Phys. **B205**[FS5], 545 (1982).
[84]R. C. Brower, M. Creutz, and M. Nauenberg, Nucl. Phys. **B210**[FS6], 133 (1982).
[85]H. Hamber and G. Parisi, Phys. Rev. Lett. **47**, 1792 (1981).
[86]B. Berg, A. Billoire, and C. Rebbi, Ann. Phys. (NY) **142**, 185 (1982).
[87]M. Falcioni, E. Marinari, M. L. Paciello, G. Parisi, R. Rapuano, B. Taglienti, and Y. Zhang, Phys. Lett. **B110**, 295 (1982); Nucl. Phys. **B215**[FS7], 265 (1983).
[88]K. Ishikawa, M. Teper, and G. Schierholz, Phys. Lett. **B110**, 399 (1982).
[89]B. Berg and A. Billoire, Phys. Lett. **B113**, 65 (1982).
[90]B. Berg and A. Billoire, Phys. Lett. **B114**, 324 (1982).
[91]K. Ishikawa, M. Teper, and G. Schierholz, Phys. Lett. **B116**, 429 (1982).
[92]K. Ishikawa, M. Teper, and G. Schierholz, Z. Phys. **C16**, 69 (1982).
[93]K. Ishikawa, A. Sato, G. Schierholz, and M. Teper, Phys. Lett. **B120**, 387 (1983).
[94]B. Berg and A. Billoire, Nucl. Phys. **B221**, 109 (1983); **B226**, 405 (1983).
[95]K. Ishikawa, G. Schierholz, and M. Teper, Z. Phys. **C19**, 327 (1983); K. Ishikawa, A. Sato, G. Schierholz, and M. Teper, Z. Phys. **C21**, 167 (1983).
[96]K. H. Mütter and K. Schillinger, Phys. Lett. **B117**, 75 (1982).
[97]K. H. Mütter and K. Schillinger, Phys. Lett. **B121**, 267 (1983).
[98]C. Michael and I. Teasdale, Nucl. Phys. **B215**[FS7], 433 (1983).
[99]L. McLerran and B. Svetitsky, Phys. Lett. **B98**, 195 (1981); Phys. Rev. **D24**, 450 (1981).
[100]J. Kuti, J. Polónyi, and K. Szlachány, Phys. Lett. **B98**, 199 (1981).
[101]J. Engels, F. Karsch, H. Satz, and I. Montvay, Phys. Lett. **B101**, 89 (1981).
[102]K. Kajantie, C. Montonen, and E. Pietarinen, Z. Phys. **C9**, 253 (1981).
[103]I. Montvay and E. Pietarinen, Phys. Lett. **B110**, 148 (1982); **115**, 151 (1982).
[104]J. Kogut, M. Stone, H. W. Wyld, W. R. Gibbs, J. Shigemitsu, S. H. Shenker, and D. K. Sinclair, Phys. Rev. Lett. **50**, 393 (1983).
[105]R. V. Gavai, Nucl. Phys. **B215**[FS7], 458 (1983).
[106]R. Gavai, F. Karsch, and H. Satz, Nucl. Phys. **B220**[FS8], 223 (1983).
[107]W. E. Caswell, Phys. Rev. Lett. **33**, 244 (1974); D. R. T. Jones, Nucl. Phys. **B75**, 531 (1974).
[108]A. J. Buras, in: Proceedings of the 1981 International Symposium on Lepton and Photon Interactions at High Energies, Bohn, 1981, p. 636.
[109]G. Münster, Phys. Lett. **B95**, 59 (1980); Nucl. Phys. **B180**[FS2], 23 (1981); J. P. Kowall and H. Neuberger, Phys. Lett. **B189**, 535 (1981).
[110]J. B. Kogut, R. B. Pearson, and J. Shigemitsu, Phys. Rev. Lett. **43**, 484 (1979); G. Münster and P. Weisz, Phys. Lett. **B96**, 119 (1980).
[111]C. B. Lang and C. Rebbi, Phys. Lett. **B115**, 137 (1982).
[112]J. B. Kogut, D. K. Sinclair, R. B. Pearson, J. L. Richardson, and J. Shigemitsu, Phys. Rev. **D23**, 2945 (1981).
[113]A. Hasenfratz, E. Hasenfratz, and P. Hasenfratz, Nucl. Phys. **B180**[FS2], 353 (1981); C. Itzykson, M. Peskin, and J. B. Zuber, Phys. Lett. **B95**, 259 (1980); M. Lüscher, G. Münster, and P. Weisz, Nucl. Phys. **B180**[FS2], 1 (1981).
[114]J. D. Stack, Phys. Rev. **D27**, 412 (1983).
[115]B. Berg and J. Stehr, Z. Phys. **C9**, 333 (1981).
[116]C. B. Lang, C. Rebbi, P. Solomonson, and R.-S. Skagerstam, Phys. Lett. **B101**, 173 (1981).
[117]M. Creutz, Phys. Rev. **D23**, 1815 (1981).
[118]R. W. B. Ardill, M. Creutz, and K. J. M. Moriarty, Phys. Rev. **D27**, 1956 (1983).
[119]L. P. Kadanoff, Ann. Phys. (NY) **100**, 359 (1976).
[120]S. Caracciolo and P. Menotti, Nucl. Phys. **B180**[FS2], 428 (1981); M. Nauenberg and D. Toussaint, Nucl. Phys. **B190**[FS3], 217 (1981).
[121]E. Pietarinen, Nucl. Phys. **B190**[FS3], 349 (1981).
[122]E.-M. Ilgenfritz and M. Mueller-Preussker, Z. Phys. **C16** 339 (1983).
[123]M. S. Marinov, Usp. Fiz. Nauk **121**, 377 (1977) [Sov. Phys. Usp. **20**, 179 (1977)].
[124]E. Eichten, K. Gottfried, T. Kinoshita, K. D. Lane, and T. M. Yan, Phys. Rev. **D21**, 203 (1980).
[125]A. Hasenfratz and P. Hasenfratz, Phys. Lett. **B93**, 165 (1980).
[126]G. 't Hooft, Nucl. Phys. **B72**, 461 (1974).
[127]A. Patkos, Phys. Lett. **B110**, 391 (1982).
[128]J. Kogut, D. K. Sinclair, and L. Susskind, Nucl. Phys. **B114**, 199 (1976); G. Münster, Nucl. Phys. **B190**[FS3], 439 (1981); **B200**[FS4], 536 (*E*) (1982); **B205**[FS5], 545 (*E*) (1982); J. Smit, **B206**, 309 (1982); G. Münster, Preprint BUTP-21/1982, Bern, 1982.
[129]A. M. Polyakov, Phys. Lett. **B72**, 477 (1978); L. Susskind, Phys. Rev. **D20**, 2610 (1979).
[130]E. L. Feĭnberg, Usp. Fiz. Nauk **139**, 3 (1983) [Sov. Phys. Usp. **26**, 1 (1983)].
[131]R. Dashen and D. J. Gross, Phys. Rev. **D23**, 2340 (1981).
[132]C. B. Lang, C. Rebbi, P. Solomonson, and B.-S. Skagerstam, Phys. Rev. **D26**, 2028 (1982); A. Gonzales-Arroyo and C. P. Korthals-Altes, Nucl. Phys. **B205**[FS5], 46 (1982); A. DiGiacomo and G. Paffuti, Nucl. Phys. **B205**[FS5], 313 (1982).
[133]G. Bhanot and R. Dashen, Phys. Lett. **B113**, 229 (1982).
[134]H. S. Sharatchandra and P. H. Weisz, DESY Preprint 81-083, 1981.
[135]N. S. Manton, Phys. Lett. **B96**, 328 (1980).
[136]J. M. Drouffe, Phys. Rev. **D18**, 1174 (1978); P. Menotti and E. Onofri, Nucl. Phys. **B190**[FS3], 288 (1981).
[137]A. Gonzales-Arroyo, C. P. Korthals-Altes, J. Peiro, and M. Perrottet, Phys. Lett. **B116**, 414 (1982).
[138]F. Gliozzi, F. Ravanini, and S. Scinto, Phys. Lett. **B118**, 402 (1982).
[139]B. Grossman and S. Samuel, Phys. Lett. **B120**, 383 (1982).
[140]Yu. M. Makeenko, M. I. Polikarpov, and A. V. Zhelonkin, Phys. Lett. **B126**, 82 (1983).
[141]A. Di Giacomo and G. C. Rossi, Phys. Lett. **B100**, 481 (1981); J. Kripfganz, Phys. Lett. **B101**, 169 (1981); A. Di Giacomo and G. Paffuti, Phys. Lett. **B108**, 327 (1981); R. Kirschner, J. Kripfganz, J. Ranft, and A. Schiller, Nucl. Phys. **B210**[FS6], 567 (1982); K. Ishikawa, G. Schierholz, H. Schneider, and M. Teper, Nucl. Phys. **B227**, 221 (1983).
[142]T. Banks, R. Horsley, H. R. Rubinstein, and V. Wolff, Nucl. Phys. **B19**[FS3], 692 (1981); E. M. Ilgenfritz, M. Müller-Preussker, Phys. Lett. **B119**, 395 (1982).
[143]P. Di Vecchia, K. Fabricius, G. C. Rossi, and G. Veneziano, Nucl. Phys. **B192**, 392 (1981); Phys. Lett. **B108**, 323 (1982).
[144]N. V. Makhaldiani and M. Müller-Preussker, Pis'ma Zh. Eksp. Teor. Fiz. **37**, 440 (1983) [JETP Lett. **37**, 523 (1983)]; K. Fabricius and G. C. Rossi, Phys. Lett. **B127**, 229 (1983).
[145]F. Fucito, E. Marinari, G. Parisi, and C. Rebbi, Nucl. Phys. **B180**[FS2], 369 (1981); D. Weingarten and D. Petcher, Phys. Lett. **B99**, 333 (1981); D. L. Scalapino and R. L. Sugar, Phys. Rev. Lett. **46**, 519 (1981); E. Marinari, G. Parisi, and C. Rebbi, Nucl. Phys. **B190**[FS3], 734 (1981); A. Duncan and M. Furman, Nucl. Phys. **B190**[FS3], 767 (1981); H. Hamber, Phys. Rev. **D24**, 951 (1981).

[146]E. Marinari, G. Parisi, and C. Rebbi, Phys. Rev. Lett. **47**, 1795 (1981); D. H. Weingarten, Phys. Lett. **B109**, 57 (1982); H. Hamber, E. Marinari, G. Parisi, and C. Rebbi, Phys. Lett. **B108**, 314 (1982).
[147]A. Hasenfratz, Z. Kunszt, P. Hasenfratz, and C. B. Lang, Phys. Lett. **B110**, 289 (1982); **B117**, 81 (1982).
[148]F. Fucito, G. Martinelli, C. Omero, G. Parisi, R. Petronzio, and F. Rapuano, Nucl. Phys. **B210**[FS6], 407 (1982); D. Weingarten, Nucl. Phys. **B215**[FS7], 1 (1983); H. Hamber and G. Parisi, Phys. Rev. **D27**, 208 (1983); C. Bernard, T. Draper, and K. Olynyk, Phys. Rev. **D27**, 227 (1983); H. Lipps, G. Martinelli, R. Petronzio, and F. Rapuano, Phys. Lett. **B126**, 250 (1983); H. W. Hamber, Phys. Rev. **D27**, 2239 (1983).
[149]M. Fukugita, T. Kaneko, and A. Ukawa, Nucl. Phys. **B230**[FS10], 62 (1982).
[150]A. Duncan, R. Roskies, and H. Vaidya, Phys. Lett. **B114**, 439 (1982).
[151]H. W. Hamber, E. Marinari, G. Parisi, and C. Rebbi, Phys. Lett. **B124**, 99 (1983).
[152]W. Duffy, G. Guralnik, and D. Weingarten, Phys. Lett. **B125**, 311 (1983).
[153]P. Hasenfratz and I. Montvay, Phys. Rev. Lett. **50**, 309 (1983).
[154]M. Fukugita, M. Kaneko, and A. Ukawa, Phys. Rev. **D27**, 2696 (1983); F. Gutbord, P. Hasenfratz, Z. Kunszt, and I. Montvay, Phys. Lett. **B128**, 415 (1983); G. Parisi, R. Petronzio, and F. Rapuano, Phys. Lett. **B128**, 418 (1983); A. Patel and R. Gupta, Caltech Preprint 68-973, Vol. 135, 1983, p. 133; J. D. Stack, Santa Barbara Preprint NSF, ITP-83-136, 1983.
[155]Yu. M. Makeenko and M. I. Polikarpov, Pis'ma Zh. Eksp. Teor. Fiz. **38**, 403 (1983) [JETP Lett. **38**, 489 (1983)]; Phys. Lett. B, [**sic**] (1984).

Translated by Dave Parsons